Effect of Electrical Modification of Cardiomyocytes on Transcriptional Activity through 5′-AMP-activated Protein Kinase

Yoshihiko Kakinuma, Yanan Zhang†, Motonori Ando*, Tetsuro Sugiura†, and Takayuki Sato**

Abstract: Endothelin-1 (ET-1) is known as an aggravating factor of the failing cardiomyocytes and, therefore, a therapeutic method is indispensable to decrease cardiac ET-1 expression. To study the mechanisms of how cardiac ET-1 gene expression can be modified, we investigated the effect of electrical stimulation against cardiomyocytes. Considering the physiology of cardiomyocytes, in vitro cultured cardiomyocytes demonstrate distinctive features from in vivo cardiomyocytes (i.e. the absence of a stretch along with electrical stimulation). In this study, we especially focused on the effect of electrical stimulation. The electrical stimulation reduced the gene expression of ET-1 mRNA in rat primary cultured cardiomyocytes. Furthermore, this effect on the transcriptional modification of ET-1 was also identified in H9c2 cells. Luciferase activity using H9c2 cells was decreased by electrical stimulation in the early phase, suggesting that the attenuation of the ET-1 gene transcription by electrical stimulation should be due to a transcriptional repression. To further investigate a trigger signal involved in the transcriptional repression, phosphorylation of 5′-AMP-activated protein kinase (AMPK) was evaluated. It was revealed that AMPK was phosphorylated in the early phase of electrical stimulation of H9c2 cells as well as in rat primary cultured cardiomyocytes, and that AMPK phosphorylation was followed by ET-1 transcriptional repression, suggesting that electrical stimulation directly regulates AMPK. This study suggests that AMPK activation in cardiomyocytes plays a crucial role in the transcriptional repression of ET-1.

Key Words: endothelin-1, cardiomyocytes, 5′-AMP-activated protein kinase

(*J Cardiovasc Pharmacol*™ 2004;44(suppl 1):S435–S438)

The endothelin (ET) system is known to be indispensable for the development of the heart. In the developmental stage, ET-1 exerts the formation of the heart through the receptors endothelin-A and endothelin-B, and the system exerts the biological function through either autocrine or paracrine fashion. It has been reported that deformity of the heart is produced in the absence of the ET system. Especially, cardiomyocytes have been reported to remarkably express and produce ET-1 in the pathophysiological condition (i.e. the failing heart) compared with the normal heart.[1] The mechanisms have been extensively studied of how the failing heart expresses ET-1 in the progression of heart failure; however, our previous study clearly demonstrated one aspect of the mechanisms — impaired cardiac energy metabolism.[2] The level of cardiac ET-1 gene expression is dependent on the condition of the cardiomyocytes in vivo; the failing cardiomyocytes produce more ET-1. However, even normal primary cultured cardiomyocytes in vitro could extraordinarily express ET-1 compared with in vivo. The abnormal pattern of cardiac ET-1 gene expression in vitro is also accompanied with a surprising switch of the myosin heavy chain isoform from α to β (a fetal pattern), suggesting that our cultured cardiomyocytes have already biologically changed their character.[3] However, this finding might provide us with some therapeutic clue as to how cardiac ET-1 expression can be depressed using cultured cardiomyocytes. If we could obtain some tool to repress cardiac ET-1 gene expression in vitro, it might lead to clarification of one of the therapeutic strategies against heart failure. Consequently we have so far concentrated on searching for ways to decrease cardiac ET-1 gene expression. Among them, we have found several methods to modify the expression using not chemicals or drugs, but physical stimulation.[3] In this study, using electrical stimulation (ES) we have successfully inhibited the cardiac ET-1 gene expression, and investigated the mechanisms by which such stimulation causes a depression of the gene expression.

METHODS

Cell Culture of Rat Cardiomyocytes and H9c2 Cells

According to our previous studies,[1] cardiomyocytes were isolated from 2-day-old Wistar–Kyoto rats. 5-Aminoimidazole-4-carboxamide-1-β-D-ribofuranosyl 5-monophosphate (AICAR) was purchased from Sigma (St Louis, MO, U.S.A.), and H9c2 cells were transiently treated by AICAR.

*Department of Cardiovascular Control and †Department of Laboratory Medicine, Kochi Medical School, Nankoku, Kochi, Japan
Address correspondence and reprint requests to Yoshihiko Kakinuma, Department of Cardiovascular Control, Kochi Medical School, Kohasu, Nankoku-shi, Kochi-ken 783-8505, Japan. E-mail: kakinuma@med.kochi-u.ac.jp
This study was supported by a Health and Labor Sciences Research Grant (H14-NANO-002) for Advanced Medical Technology from the Ministry of Health, Labor, and Welfare of Japan.

Electrical Stimulation

We have developed a specific ES device, which is modified to simultaneously provide multi-channels of ES and also to efficiently regulate bidirectional current. Our protocol for ES was performed as follows: 10 V, 10 milliseconds of duration and 4 Hz of frequency.

RNA Isolation and Reverse Transcription-Polymerase Chain Reaction

As previously described, total RNA was isolated, and 1 μg total RNA was reverse-transcribed and used for a polymerase chain reaction (PCR) template. PCR primers were prepared for preproET-1, hypoxia-inducible factor (HIF)-1α, β-actin,[2,3] and glucose transporter 3.

Luciferase Assay

As previously reported, the 5′-regulatory region of preproET-1 gene was subcloned into a luciferase vector.[2] The reporter vector was transfected into H9c2 cells by a cationic reagent, Effecten (QIAGEN, Valencia, CA, U.S.A.), according to the manufacture's protocol. Forty-eight hours after transfection, cells were lysed for evaluation of luciferase activity.

Western Blot Analysis

Cells were harvested from dishes by scraping, were washed with phosphate-buffered saline, and cell lysates were mixed with sample buffer. The samples were fractionated by sodium dodecyl sulfate-polyacrylamide gel electrophoresis and transferred onto membranes (Millipore Corp., Bedford, MA, U.S.A.). After transfer into the membrane, they were soaked in blocking buffer. The membranes were incubated with a monoclonal phosphor-5′-AMP-activated protein kinase-α (Thr172) antibody (1:1000; Cell Signaling Technology, Beverly, MA, U.S.A.). After the membranes were washed, horseradish peroxidase-conjugated secondary antibodies (Promega, Madison, WI, U.S.A.) were applied and the signal was detected using an enhanced chemi-luminescence system (Amersham, Piscataway, NJ, U.S.A.).

RESULTS

Electrical Stimulation Affects Gene Expression of Rat Cardiomyocytes

To investigate transcriptional regulation of cardiomyocytes, primary cultured cardiomyocytes were subjected to ES. Even with a bi-directional current, cardiomyocytes could not be cultured for ES more than 16 hours. As demonstrated in Fig. 1, ES remarkably decreased gene expression of preproET-1 and HIF-1α in the cardiomyocytes, compared with non-stimulated cardiomyocytes. However, the mRNA level of β-actin was not decreased by ES. Adversely, gene expression of glucose transporter 3 mRNA was increased by ES. These results suggested that

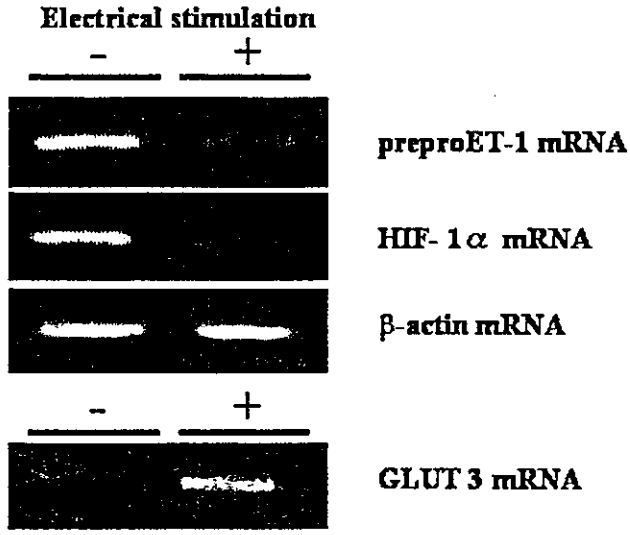

FIGURE 1. Electrical stimulation (ES) modifies gene expression of preproendothelin-1 (preproET-1), hypoxia-inducible factor-1α (HIF-1α), and glucose transporter (GLUT) 3 mRNAs. PreproET-1 and HIF-1α gene expressions were decreased 5 hours after ES. In contrast, GLUT 3 gene expression was increased by ES. The level of β-actin mRNA was not affected by ES.

cardiomyocytes respond to ES with an increased gene expression of glucose transporter 3; however, in contrast, such an ES modified gene expression of cardiac preproET-1 and HIF-1α.

Electrical Stimulation Transcriptionally Regulates PreproET-1 Gene Expression

Further to investigate especially the gene expression of preproET-1 mRNA, a reporter assay was performed using a reporter vector possessing the 5′-promoter regulatory region of the preproET-1 gene. H9c2 cells, a cell line of rat ventricular cardiomyocytes, were transfected by the reporter vector. As shown in Fig. 2, ES of H9c2 cells greatly decreased the luciferase activity of preproET-1. The phenomenon of the depressed luciferase activity was compatible with the decreased preproET-1 mRNA by reverse transcription-PCR.

Electrical Stimulation Elevates Phosphorylation of 5′-AMP-activated Protein Kinase

To investigate mechanisms to decrease a transcriptional level of preproET-1, we studied whether ES activates the phosphorylation of 5′-AMP-activated protein kinase (AMPK) using H9c2 cells. The time course study demonstrated that AMPK phosphorylation was detected soon after ES (Fig. 3). Furthermore, such an increase in AMPK phosphorylation was also observed in primary cultured cardiomyocytes. It was suggested that ES causes activation of

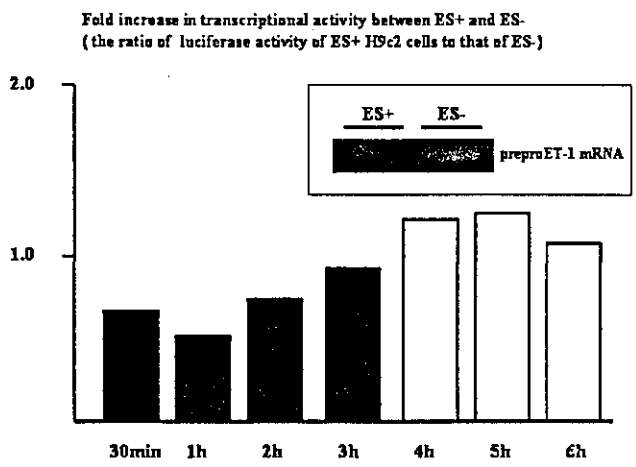

FIGURE 2. Electrical stimulation (ES) transcriptionally represses preproendothelin-1 (preproET-1) gene expression in H9c2 cells. Gene expression of preproET-1 in H9c2 cells was also decreased by ES. Using a reporter vector of the preproET-1 gene, luciferase activity was compared between electrical stimulated (ES+) H9c2 cells and non-electrical stimulated (ES–) cells. The ratio of luciferase activity of ES+ to that of ES– was measured, where a ratio > 1 suggests transcriptional activation, contrasting with a ratio < 1 suggesting repression.

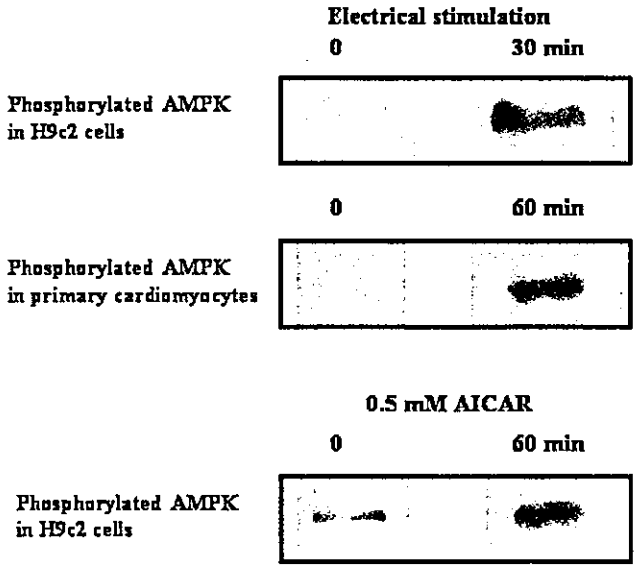

FIGURE 3. 5'-AMP-activated protein kinase (AMPK) is activated through phosphorylation by electrical stimulation (ES). ES caused activation of AMPK through phosphorylation in H9c2 cells. This phenomenon was also detected in rat primary cultured cardiomyocytes with a comparable time course. Also, 0.5 m*M* 5-aminoimidazole-4-carboxamide-1-β-D-ribofuranosyl 5-monophosphate (AICAR), an activator of AMPK, phosphorylated AMPK.

AMPK with a comparable time course of suppression of the preproET-1 gene, and consequently that AMPK phosphorylation is profoundly related to the repression of transcriptional activity of preproET-1 gene expression.

An Activator of AMPK Causes a Decrease in PreproET-1 mRNA

H9c2 cells were treated by AICAR, which is known as an activator of AMPK. As demonstrated in Fig. 3, AICAR increased the phosphorylation of AMPK. The activation of AMPK occurred very rapidly with a comparable time course of ES. With treatment of AICAR, the mRNA level of preproET-1 was decreased (Fig. 4). It was suggested that AMPK activation was involved in the attenuated preproET-1mRNA gene expression.

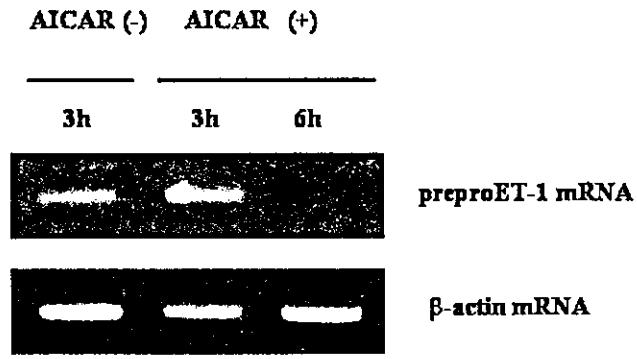

FIGURE 4. 5'-AMP-activated protein kinase activator decreases preproendothelin-1 (preproET-1) gene expression in H9c2 cells. 5-Aminoimidazole-4-carboxamide-1-β-D-ribofuranosyl 5-monophosphate (AICAR) 1.5 m*M* treatment remarkably decreased the gene expression of preproET-1 mRNA in H9c2 cells.

DISCUSSION

ET-1 is one of the aggravating factors in heart failure, because ET-1 further activates the glycolytic system in the failing cardiomyocytes, resulting in aggravation of malfunction in the heart. Therefore, one of the therapeutic goals that inhibit the progression of heart failure might be to decrease cardiac ET-1 gene expression. There are many manipulations to decrease ET-1 gene expression, including blocking the renin–angiotensin system and ET receptor antagonists.[4] However, we have further investigated whether other manipulations can modify the cardiac ET-1 expression, and then finally we have identified that a mechanical stimulation (i.e. ES) decreases cardiac ET-1 expression through activation of AMPK.

AMPK is known as a fuel sensor kinase, which is activated through phosphorylation when a cellular adenosine triphosphate (ATP) level is decreased.[5] Consequently, cells respond to a shortage of the energy and activate the

phosphorylation of AMPK. This kinase is therefore activated in the early phase to stimuli that might cause mitochondrial dysfunction, leading to ATP deprivation. This response through AMPK phosphorylation is considered an adaptation of cells to avoid cellular death with a shortage of ATP. However, this response is not only involved in pathological states, but also in physiological states. For example, exercise-induced muscle hypertrophy leads to remarkable adaptation of the muscle to the more efficient utilization of energy (i.e. mitochondrial β-oxidation of fatty acid), and consequently to activation of the mitochondrial function.[6] In the case of exercise, AMPK in skeletal muscle is known to be activated.[7] Therefore, it is suggested that the activation of AMPK through phosphorylation is followed by enhancement of mitochondrial function in a physiological condition to obtain more adequate ATP.

It is known that the cardiomyocytes obtain ATP predominantly through mitochondrial β-oxidation of fatty acid; however, when cardiomyocytes were treated by hypoxia, the cardiac energy metabolic system was changed from β-oxidation to glycolysis, because fatty acid oxidation is impaired. In such a case, as our previous study demonstrated, HIF-1α is induced for upregulation of glycolytic enzymes, and furthermore HIF-1α transcriptionally activates preproET-1 gene expression in the failing heart.[2] It is suggested that cardiac ET-1 expression is accompanied with a cellular glycolysis-dominant energy system.[8] With these findings in mind, further speculation is as follows: if the glycolysis-dominant energy system is inhibited, and alternatively mitochondrial β-oxidation of fatty acid is activated, ET-1 gene expression could be decreased. As our present study demonstrated, ES activates the phosphorylation of AMPK in a rapid fashion, followed by a decrease in the transcriptional activity of ET-1.

This is a first demonstration of transcriptional repression of cardiac preproET-1 gene expression using methods other than drugs. Moreover, this reaction is very rapid to decrease preproET-1 mRNA. Therefore, it is suggested that the manipulation of cardiomyocytes by ES is one candidate method to inhibit an increase in cardiac ET-1 gene expression.

REFERENCES

1. Kakinuma Y, Miyauchi T, Kobayashi T, et al. Myocardial expression of endothelin-2 is altered reciprocally to that of endothelin-1 during ischemia of cardiomyocytes *in vitro* and during heart failure *in vivo*. *Life Sci.* 1999;65:1671–1683.
2. Kakinuma Y, Miyauchi T, Yuki K, et al. Novel molecular mechanism of increased myocardial endothelin-1 expression in the failing heart involving the transcriptional factor hypoxia inducible factor-1α induced for impaired myocardial energy metabolism. *Circulation.* 2001;103: 2387–2394.
3. Kakinuma Y, Miyauchi T, Suzuki T, et al. Enhancement of glycolysis in cardiomyocytes elevates endothelin-1 expression through the transcriptional factor HIF-1α. *Clin Sci.* 2002;103(suppl. 48):210S–214S.
4. Sakai S, Miyauchi T, Kobayashi T, et al. Inhibition of myocardial endothelin pathway improves lomg-term survival in heart failure. *Nature.* 1996;384:353–355.
5. Winder WW. Energy-sensing and signaling by AMP-activated protein kinase in skeletal muscle. *J Appl Physiol.* 2001;91:1017–1028.
6. Saha AK, Schwarsin AJ, Roduit R, et al. Activation of malonyl-CoA decarboxylase in rat skeletal muscle by contraction and the AMP-activated protein kinase activator 5-aminoimidazole-4-carboxamide-1-β-D-ribofuranoside. *J Biol Chem.* 2000;275:24279–24283.
7. Hood DA. Plasticity in skeletal, cardiac, and smooth muscle invited review: contractile activity-induced mitochondrial biogenesis in skeletal muscle. *J Appl Physiol.* 2001;90:1137–1157.
8. Wu-Wong JR, Berg CE, Kramer D. Endothelin stimulates glucose uptake via activation of endothelin-A receptor in neonatal rat cardiomyocytes. *J Cardiovasc Pharmacol.* 2000;36(5 suppl. 1): S179–S183.

Overexpression of Inducible Nitric Oxide Synthase in Rostral Ventrolateral Medulla Causes Hypertension and Sympathoexcitation via an Increase in Oxidative Stress

Yoshikuni Kimura, Yoshitaka Hirooka, Yoji Sagara, Koji Ito, Takuya Kishi, Hiroaki Shimokawa, Akira Takeshita, Kenji Sunagawa

Abstract—The present study examined the role of inducible nitric oxide synthase (iNOS) in the rostral ventrolateral medulla (RVLM) of the brain stem, where the vasomotor center is located, in the control of blood pressure and sympathetic nerve activity. Adenovirus vectors encoding iNOS (AdiNOS) or β-galactosidase (Adβgal) were transfected into the RVLM in Wistar-Kyoto (WKY) rats. Blood pressure and heart rate were monitored using a radiotelemetry system. iNOS expression in the RVLM was confirmed by immunohistochemical staining or Western blot analysis. Mean arterial pressure significantly increased from day 6 to day 11 after AdiNOS transfection, but did not change after Adβgal transfection. Urinary norepinephrine excretion was significantly higher in AdiNOS-transfected rats than in Adβgal-transfected rats. Microinjection of aminoguanidine or *S*-methylisothiourea, iNOS inhibitors, or tempol, an antioxidant, significantly attenuated the pressor response evoked by iNOS gene transfer. The levels of thiobarbituric acid-reactive substances, a marker of oxidative stress, were significantly greater in AdiNOS-transfected rats than in Adβgal-transfected rats. Dihydroethidium fluorescence in the RVLM was increased in AdiNOS-transfected rats. In addition, nitrotyrosine-positive cells were observed in the RVLM only in AdiNOS-transfected rats. Intracisternal infusion of tempol significantly attenuated the pressor response and the increase in the levels of thiobarbituric acid–reactive substances induced by AdiNOS transfection. These results suggest that overexpression of iNOS in the RVLM increases blood pressure via activation of the sympathetic nervous system, which is mediated by an increase in oxidative stress. (*Circ Res.* 2005;96:252-260.)

Key Words: nitric oxide synthase ■ blood pressure ■ sympathetic nervous system ■ oxidative stress ■ gene transfer

Nitric oxide (NO) in the central nervous system (CNS), including the brain stem and hypothalamus, plays an important role in the regulation of blood pressure via the sympathetic nervous system.[1-7] In general, NO in the CNS inhibits sympathetic nerve activity, thereby reducing blood pressure.[2-4] The rostral ventrolateral medulla (RVLM) in the brain stem contains sympathetic premotor neurons responsible for maintaining the tonic excitation of sympathetic preganglionic neurons involved in cardiovascular regulation.[8-10] The functional integrity of the RVLM is essential for the maintenance of basal vasomotor tone, and RVLM abnormalities might be related to the pathophysiology of hypertension[11-14] and heart failure.[15,16]

Recently, we developed a technique for adenovirus-mediated endothelial NO synthase (eNOS) gene transfer into the RVLM[11,14,17-19] or the nucleus tractus solitarii (NTS)[20,21] in vivo. An increase in NO production in the RVLM induced by eNOS overexpression decreases blood pressure and heart rate (HR) by inhibiting the sympathetic nervous system.[11,14,19] In that series of studies, we used eNOS instead of neuronal NO synthase (nNOS), which is normally abundant in the CNS, because the purpose of the study was to examine the effect of an increase in NO production in the RVLM on cardiovascular function. There are three types of NOS: eNOS, nNOS, and inducible NOS (iNOS). eNOS and nNOS are constitutively expressed, but iNOS is expressed only during pathophysiological states such as hypertension, heart failure, and endotoxin shock, and in aging.[22-28]

The aim of the present study was to examine the effect of iNOS overexpression in the RVLM on blood pressure in vivo and to determine whether an increase in oxidative stress in the RVLM is involved in blood pressure changes. For this purpose, we transfected adenovirus encoding the iNOS gene (AdiNOS) into the RVLM and monitored mean arterial pressure (MAP) and HR using a radiotelemetry system in awake rats. NO activity is determined by the balance of NO and reactive oxygen species production.[23] Therefore, thiobarbituric acid–reactive substances (TBARS) in the RVLM were measured as an indirect marker of oxidative stress,[29,30] and tempol, a superoxide dismutase mimetic,[29,30] was microin-

Original received July 26, 2004; revision received November 9, 2004; accepted November 29, 2004.

From the Department of Cardiovascular Medicine, Kyushu University Graduate School of Medical Sciences, Fukuoka, Japan.

Correspondence to Yoshitaka Hirooka, MD, PhD, FAHA, Department of Cardiovascular Medicine, Kyushu University Graduate School of Medical Sciences, 3-1-1 Maidashi, Higashi-ku, Fukuoka 812-8582, Japan. E-mail hyoshi@cardiol.med.kyushu-u.ac.jp

Circulation Research is available at http://www.circresaha.org

DOI: 10.1161/01.RES.0000152965.75127.9d

jected bilaterally into the RVLM after transfection of AdiNOS.

Materials and Methods

General Procedures and In Vivo Gene Transfer Into the RVLM

The present study was approved by the Committee on Ethics of Animal Experiments, Faculty of Medicine, Kyushu University, and conducted according to the Guidelines for Animal Experiments of the Faculty of Medicine, Kyushu University. Male Wistar-Kyoto (WKY) rats (280 to 300 g, 16 to 20 weeks old) were used. Rats were obtained from an established colony at the Animal Research Institute of Kyushu University Faculty of Medicine (Fukuoka, Japan). Details of the general procedures of transfection of adenovirus vectors are available in the online data supplement at http://circres.ahajournals.org.

Construction of Adenovirus Vectors

We used adenoviral vectors encoding the bacterial β-galactosidase gene, mouse iNOS gene,[31,32] or bovine endothelial NOS (eNOS) gene (see online data supplement for details).[19,33]

Analysis of Gene Expression for β-Galactosidase or iNOS

At day 7 after gene transfer, β-galactosidase expression was confirmed by staining with X-Gal in phosphate buffered saline as described previously.[21] We performed double-immunohistochemical staining for iNOS and phenylethanolamine-*N*-methyltransferase (PNMT)[19] or nitrotyrosine. Details of the methods of immunohistochemistry are available in the online data supplement.

Western Blot Analysis for iNOS

To confirm the local overexpression of iNOS in the RVLM, Western blot analysis for iNOS protein from tissue containing the injection sites of the RVLM obtained using the micropunch technique[19] was performed at day 0, 3, 5, 7, 9, 11, or 14 after the gene transfer. The procedure for Western blot analysis of RVLM tissues was described previously (see online data supplement for details).[11,19]

Microinjection Into the RVLM

To confirm that changes in MAP and HR induced by AdiNOS transfection were the result of an increase in iNOS protein, we microinjected aminoguanidine (2.5 mmol/L, 50 nL per site, 250 pmol) or *S*-methylisothiourea (SMT; 2.5 mmol/L, 50 nL per site, 250 pmol) bilaterally into the RVLM at day 7 after transfection with Adβgal or AdiNOS. All injections were performed in rats anesthetized with sodium pentobarbital (50 mg/kg, IP followed by 20 mg/kg per hour, IV). A nonselective NOS inhibitor, N^G-monomethyl-L-arginine (L-NMMA), was also microinjected bilaterally into the RVLM. We microinjected L-arginine, a precursor of NO, (70 mmol/L, 50 nL per site, 7 nmol) bilaterally into the RVLM at day 7 after transfection with Adβgal or AdiNOS. To examine whether the generation of superoxide anions is involved in blood pressure alteration induced by AdiNOS transfection, microinjection of tempol, a superoxide dismutase mimetic, was performed bilaterally into the RVLM (see online data supplement for details).

Microdialysis and Measurement of NO Metabolites

We measured NO production in the RVLM as nitrite/nitrate (NOx) with in vivo microdialysis before and at day 7 after gene transfer, as described previously (see online data supplement for details).[21,34,35]

Measurement of MAP, HR, and Urinary Norepinephrine Excretion

A UA-10 telemetry system (Data Sciences International) was used to measure MAP and HR. We measured urinary norepinephrine excretion for 24 hours before the gene transfer and at day 7 after the gene transfer (see online data supplement for details).

Evaluation of Oxidative Stress in the RVLM

The RVLM tissues were homogenized in 1.15% KCl (pH 7.4), and 0.4% sodium dodecyl sulfate, 7.5% acetic acid adjusted to p 3.5 with NaOH, and 0.3% thiobarbituric acid were added to the homogenate. The amount of TBARS was determined by absorbance with a molecular extinction coefficient of 156 000 and expressed as μmol/g wet weight, as described previously (see online data supplement for details).[30] Brain superoxide anion levels were estimated in two groups of rats (AdiNOS-transfected rat, n=5; nontreated, n=5) using dihydroethidium (DHE) staining following procedures used in previous studies (see online data supplement for details).[36,37]

Continuous Intracisternal Infusion Experiments With Tempol

The rats were randomly divided into four groups. Two of the groups were transfected with AdiNOS and two of the groups with Adβgal. Either vehicle (artificial cerebrospinal fluid, aCSF) or tempol (12 μmol/d) were continuously infused intracisternally (0.25 μL/h) for 1 week with an osmotic minipump (Alzet model 1002; DURECT Corporation), as described previously (see online data supplement for details).[38,39] Half of the animals in each transfection group were infused with vehicle and the other half were infused with tempol, producing four groups of animals: AdiNOS-VEH, AdiNOS-tempol, Adβgal-VEH, and Adβgal-tempol.

Statistical Analysis

All values are expressed as mean±SEM. Two-way ANOVA was used to compare MAP, HR, and NOx levels between the AdiNOS-treated group and the other groups. Comparisons between any two mean values were performed using Bonferroni's correction for multiple comparisons. A paired *t* test was used to compare 24-hour urinary norepinephrine excretion before and at day 7 after the gene transfer. A level of $P<0.05$ was considered to be significant.

Results

Analysis of β-Galactosidase, iNOS, or Nitrotyrosine Expression

Figure 1B shows the β-galactosidase staining in a section of the rat brain medulla at day 7 after the gene transfer. A schematic representing injection site is shown in Figure 1A. β-galactosidase staining was noted in the RVLM, where Adβgal had been microinjected. There were no X-Gal–positive cells in the adjacent brain regions. In the AdiNOS-transfected rats, the expression of iNOS protein was observed locally in the RVLM, where the AdiNOS had been transfected. Figures 1D, 1E, and 1F show the expression of iNOS in the RVLM at day 7 after the gene transfer by immunohistochemistry. Some of the C1 neurons labeled with the PNMT antibody were also detected with the anti-iNOS antibody (Figure 1C). The expression level of iNOS peaked at day 7 after the gene transfer and thereafter declined over time as detected by Western blot analysis (Figure 2).

Microdialysis and Measurement of NO Metabolites

We measured the production of NO in the RVLM as NOx using in vivo microdialysis before and after gene transfer. The level of NOx was significantly higher in rats transfected with AdiNOS or AdeNOS at day 7 (AdiNOS, 58.8±1.2 or AdeNOS, 29.4±1.0 pmol/20 μL, n=6 for each) than in Adβgal-treated rats (8.2±0.4 pmol/20 μL, n=6; Figure 3). NOx levels in AdiNOS-transfected rats were also significantly higher than in AdeNOS-transfected rats ($P<0.05$).

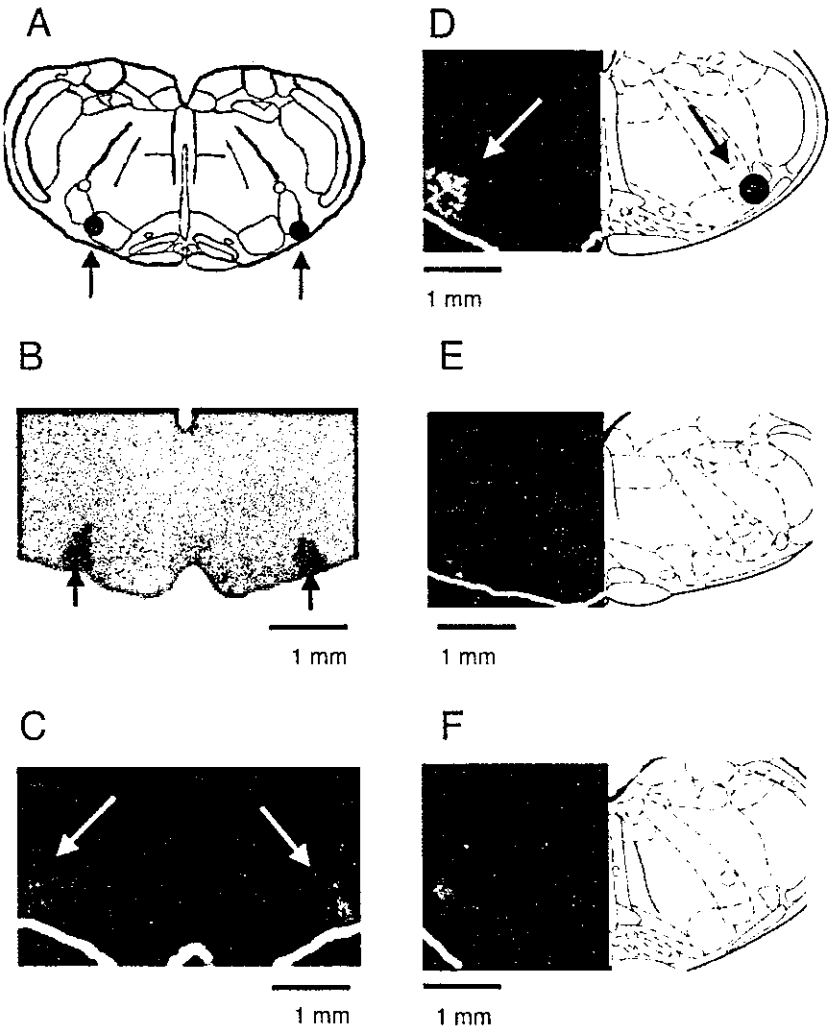

Figure 1. A, Schematic drawing of a section that includes the RVLM. Arrows indicate the RVLM. B, Site-specific expression of β-galactosidase by X-Gal staining at day 7 after gene transfer. C, Site-specific expression of PNMT by immunohistochemistry. D, Site-specific expression of iNOS protein by immunohistochemistry at day 7 after gene transfer. E, 0.5-mm rostral from the section as shown in D; F, 0.5-mm caudal from the section as shown in D. Arrows indicate the RVLM. Immunohistochemical staining for iNOS (green, visualized with fluorescein isothiocyanate-conjugated fluoroprobe) (D, E, and F) and PNMT (red, visualized with rhodamine-conjugated fluoroprobe) (C).

MAP, HR, and Urinary Norepinephrine Excretion

Figure 4A and 4B show the changes in MAP and HR before and after the gene transfer into the RVLM. MAP was significantly increased in the AdiNOS-transfected rats between days 6 and 11 after the gene transfer (+56±14 mm Hg at day 7 after the gene transfer; $P<0.05$, n=6). In contrast, MAP did not change in the Adβgal-transfected rats. Injection of AdiNOS 1 mm caudal to the RVLM also did not alter MAP. HR was not altered in either group (Figure 4B). Urinary norepinephrine excretion measured at day 7 after the gene transfer was significantly increased in the AdiNOS-transfected rats relative to that measured before gene transfer (Figure 4C). Urinary norepinephrine did not change in the Adβgal-transfected rats (Figure 4C).

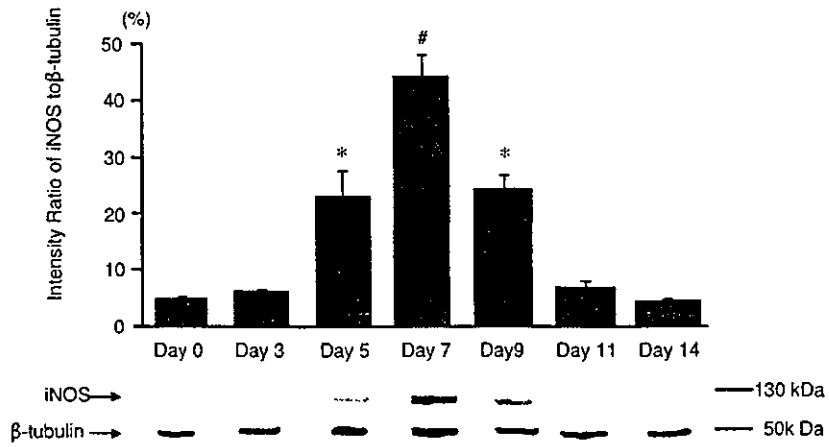

Figure 2. Representative Western blot analysis demonstrating the expression of iNOS protein, in the medulla containing the RVLM. Densitometric average was normalized to the values obtained from the analysis of β-tubulin (n=5 for each). *$P<0.05$ vs day 0. #$P<0.01$ vs day 0.

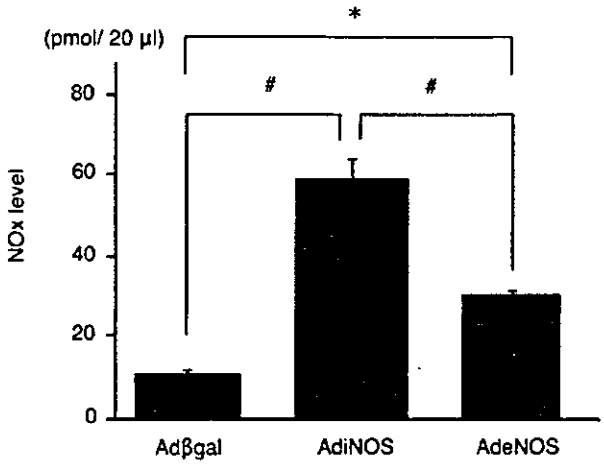

Figure 3. Effects of transfection of Adβgal (n=6), AdiNOS (n=6), and AdeNOS (n=6) into RVLM on NOx release in dialysate of the RVLM. Basal NOx levels in AdiNOS-transfected rats were significantly higher than those in Adβgal- or AdeNOS-transfected rats. Basal NOx levels in AdeNOS-transfected rats were also significantly higher than in Adβgal-transfected rats. All data are expressed as amount of NOx in 20 µL dialysate of RVLM. #$P<0.01$ compared with values of AdiNOS-transfected rats. *$P<0.05$ compared with values of Adβgal-transfected rats.

Microinjection of NOS Inhibitors Into the RVLM

Microinjection of aminoguanidine into the RVLM at day 7 after the gene transfer produced a gradual decrease in MAP in the AdiNOS-transfected rats (Figure 5A). The maximum decrease in MAP evoked by aminoguanidine was −38±12 mm Hg ($P<0.05$, n=5). In contrast, microinjection of aminoguanidine did not alter MAP in the Adβgal-transfected rats (6±4 mm Hg, $P<0.05$, n=5). Microinjection of SMT also decreased MAP in the AdiNOS-transfected rats (−42±12 mm Hg, n=5). Microinjection of L-NMMA also decreased MAP in AdiNOS-transfected rats (Figure 5B), but the change was smaller than that evoked by microinjection of aminoguanidine or SMT. In contrast, L-NMMA elicited a small but significant increase in MAP in Adβgal-transfected rats ($P<0.05$, n=3; Figure 5B).

Microinjection of L-Arginine Into the RVLM

Microinjection of L-arginine into the RVLM at day 7 after the gene transfer produced a gradual decrease in MAP in the AdiNOS-transfected rats. The maximum decrease in MAP evoked by L-arginine was −35±6 mm Hg (n=5).

Oxidative Stress in the RVLM After Gene Transfer

TBARS levels were significantly higher in the RVLM of AdiNOS-transfected rats than in Adβgal-transfected rats (Figure 6A). In AdeNOS-transfected rats, TBARS levels did not differ from those of Adβgal-transfected rats (AdeNOS, 0.32±0.03 versus Adβgal, 0.29±0.05 µmol/g, n=5 for each). Figure 6B and 6C show representative images of DHE-treated brain slices from the RVLM. Increased fluorescence, representing higher superoxide anion levels, was present in the brain slices from AdiNOS- transfected rats (Figure 6B) compared with nontreated rats (Figure 6C). Some of the iNOS-positive cells were also detected with the anti-nitrotyrosine antibody (Figure 6D and 6E). Microinjection of tempol elicited a depressor response in the AdiNOS-transfected rats, but not in the Adβgal-transfected rats (Figure 7).

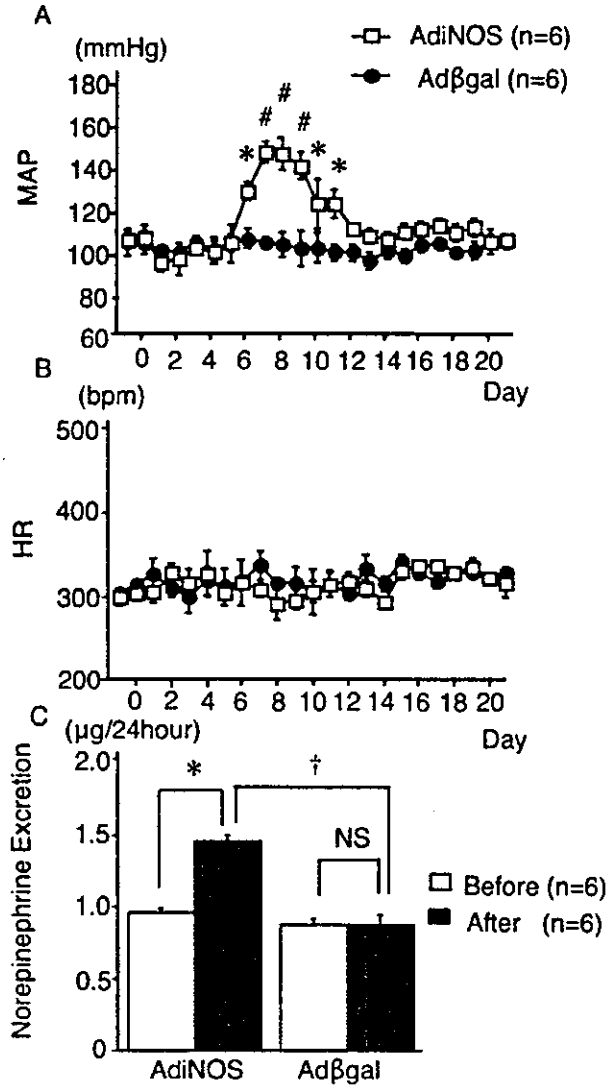

Figure 4. A and B, Time course of MAP (A, in mm Hg) and HR (B, in bpm) in Adβgal-transfected rats and AdiNOS-transfected rats before and after gene transfer. *$P<0.05$ vs the values between the two groups. #$P<0.01$ vs the values between the two groups. C, Urinary norepinephrine excretion for 24 hours (µg) before and at day 7 after the gene transfer in AdiNOS-transfected rats and Adβgal-transfected rats. *$P<0.05$, #$P<0.01$ vs the values before the gene transfer. †$P<0.05$ vs Adβgal-transfected rats. Data are shown as mean±SEM (n=6 per group).

Effect of Continuous Intracisternal Infusion With Tempol

Figure 8A shows the changes in MAP after intracisternal infusion of tempol for 1 week. Tempol significantly attenuated the increase in MAP in AdiNOS-transfected rats (Figure 8A). Urinary norepinephrine excretion measured at day 7 after the gene transfer was significantly increased in the AdiNOS-transfected rats treated with tempol relative to the AdiNOS-transfected rats treated with aCSF (Figure 8B).

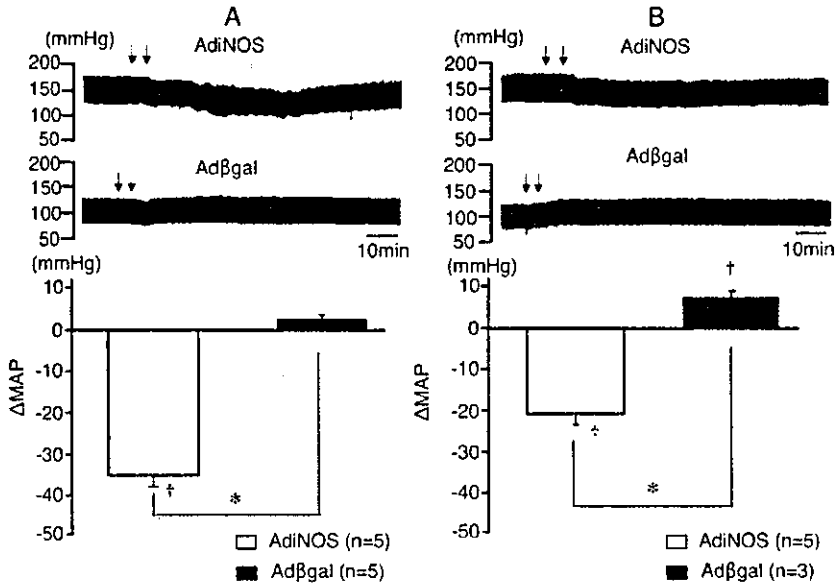

Figure 5. Changes in MAP caused by microinjection of either aminoguanidine (250 pmol) (A, n=5 for each) or L-NMMA (100 nmol) (B, n=5 for AdiNOS-transfected, n=3 for Adβgal-transfected) into the RVLM at day 7 after the gene transfer (Adβgal or AdiNOS) in anesthetized rats. Representative recordings showing blood pressure response to microinjection of aminoguanidine or L-NMMA into the bilateral RVLM at day 7 after the gene transfer. *$P<0.05$ vs the values between the two groups. †$P<0.05$ from the baseline values.

Urinary norepinephrine did not change in the Adβgal-transfected rats (Figure 8B). TBARS levels in AdiNOS-transfected rats treated with intracisternal infusion of tempol were significantly lower than in those treated with intracisternal infusion of aCSF (0.68±0.03 versus 0.52±0.03 μmol/g wet tissue; $P<0.05$, n=5 for each).

Discussion

The present study demonstrated that overexpression of iNOS in the RVLM elicits a pressor response in awake normotensive WKY rats in vivo, and that an increase in oxidative stress in the RVLM is likely to be responsible for this response. Urinary norepinephrine excretion was higher in AdiNOS-transfected rats than in Adβgal-transfected rats, indicating that it was mediated by activation of the sympathetic nervous system. In addition, the pressor response was mediated by iNOS, because aminoguanidine or SMT inhibited the response. Taken together, these results suggest that overexpression of iNOS in the RVLM causes a pressor response via activation of the sympathetic nervous system, probably attributable to an increase in oxidative stress.

Expression of iNOS protein in the RVLM was confirmed by immunohistochemistry and Western blot analysis, as shown in Figures 1 and 2. The expression level of iNOS protein after AdiNOS transfection gradually increased, peaked at day 7, and then gradually declined over time. The time course of transfected gene expression was consistent with transfected eNOS expression reported in previous studies.[11,19] To confirm the transfection site in the pressor areas in the RVLM, we identified the site functionally by prior injection of L-glutamate and anatomically by immunohistochemical staining for PNMT, which indicates the C1 area where the RVLM neurons are located.[8,19] We did not detect iNOS-positive neurons in other areas of the brain, such as the NTS, caudal ventrolateral medulla, and hypothalamus. Because of the possibility of significant diffusion to the

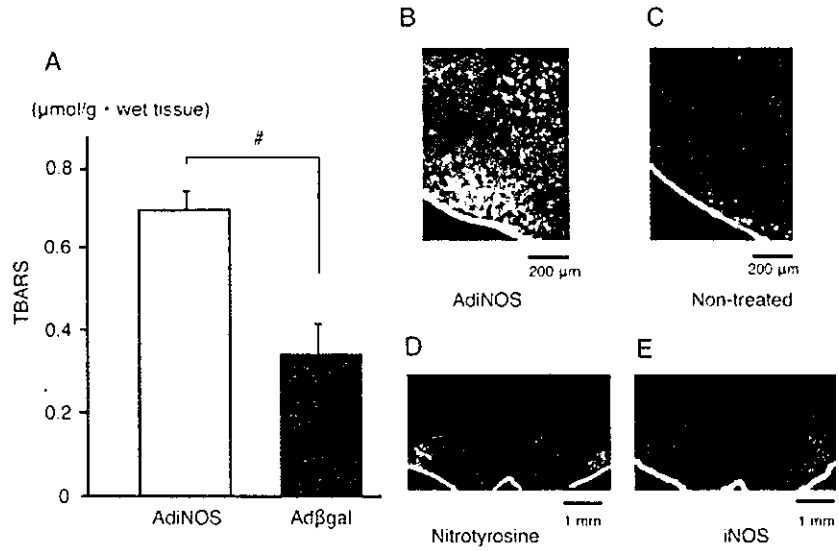

Figure 6. A, Lipid peroxidation as indicated by TBARS levels in RVLM tissues from AdiNOS-transfected rats (n=10) and Adβgal-transfected rats (n=5). #$P<0.01$. B and C, Images of dihydroethidium-treated brain slices from the RVLM from AdiNOS-transfected rats (B) and nontreated rat (C). D and E, Images of expression of nitrotyrosine (green, visualized with fluorescein isothiocyanate-conjugated fluoroprobe) (D) or iNOS protein (red, visualized with rhodamine-conjugated fluoroprobe) (E) in the RVLM.

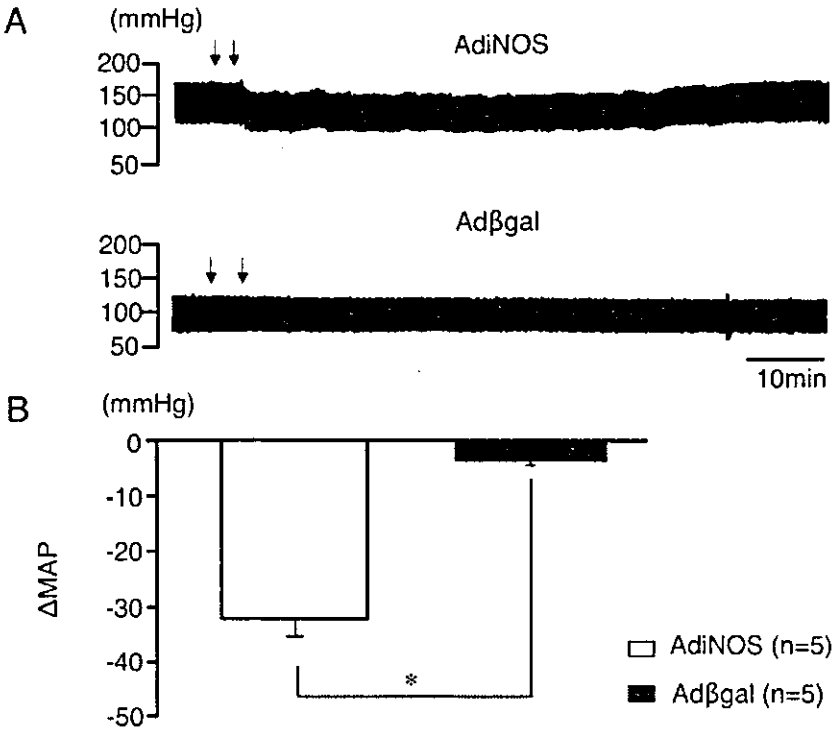

Figure 7. A, Representative recordings from AdiNOS-transfected rats and Adβgal-transfected rats showing the arterial blood pressure response to bilateral microinjections of tempol into the RVLM. Arrows indicate timing of the microinjection. B, Grouped data of MAP and HR responses evoked by microinjection of tempol into the RVLM (n=5 for each). *$P<0.05$ vs Adβgal-transfected rats.

caudal ventrolateral medulla region, which is adjacent to the RVLM, we slowly injected the adenovirus 50 nL/min with the total volume injected over 15 minutes. Thus, as shown in Figure 1D through 1F, expression of the transfected adenovirus was observed within a 1-mm wide region in the rostrocaudal direction, and there was no significant staining observed in the caudal ventrolateral medulla. Furthermore, when we injected AdiNOS 1 mm caudal to the RVLM, there were no changes in blood pressure (data not shown). There might be some cells that express iNOS, because Western blot analysis revealed a small amount of iNOS protein in the brain of WKY rats.[13] In fact, there is iNOS expression in the cerebral blood vessels (vascular smooth muscle cells) and glia (microglia and astrocytes),[40] although iNOS is normally induced by inflammatory stimuli.[40,41]

In a previous study, we reported that overexpression of eNOS in the RVLM decreases blood pressure and HR by inhibiting the sympathetic nervous system.[19] The different cardiovascular responses induced by overexpression of iNOS and eNOS might be attributable to differences in the amount of NO production.[42,43] Large amounts of NO production might consume L-arginine, a precursor of NO, thereby inducing chronic L-arginine depletion. In such conditions, iNOS produces superoxide anions instead of NO.[44,45] In the present study, the NO production measured as NOx was approximately 4.5-fold higher in AdiNOS-transfected rats than in Adβgal-transfected rats. In contrast, NOx levels in the RVLM of AdeNOS-transfected rats were approximately 2-fold higher than in Adβgal-transfected rats. This increase in basal NO production is consistent with the results of a previous study in which eNOS was transfected into the NTS[21] and of another in vivo study.[46] It is difficult, however, to explain the different effects of eNOS and iNOS overexpression in the RVLM on blood pressure based on differences in

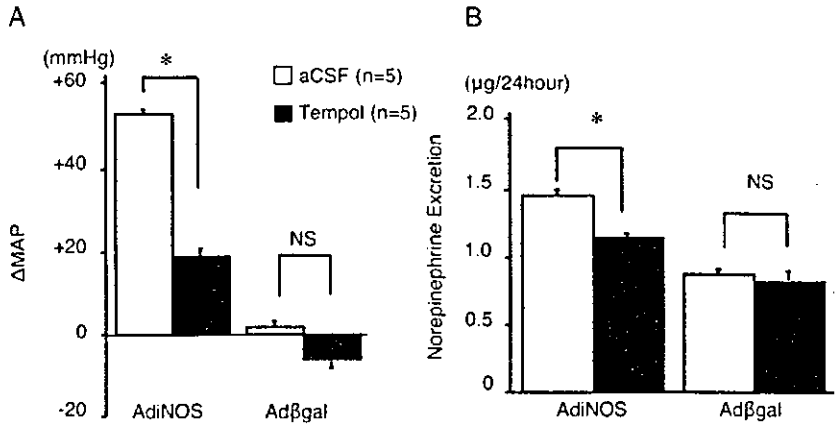

Figure 8. A, Changes in MAP caused by continuous intracisternal (i.c.) infusion with tempol (2 mol/L, 0.25 μL/h) or aCSF for 1 week (n=5 for each; Adβgal or AdiNOS). B, Urinary norepinephrine excretion for 24 hours (μg) before and at day 7 after the gene transfer in AdiNOS-transfected rats and Adβgal-transfected rats treated with tempol or aCSF (n=5 for each). *$P<0.05$ vs AdiNOS-transfected rats with aCSF.

the amount of NO release. The levels of TBARS, an indirect marker of oxidative stress in the RVLM, were higher in the AdiNOS group than in the Adβgal group. DHE staining, an oxidative fluorescent dye, detects in situ superoxide in the RVLM, and the intensity of the staining was greater in AdiNOS-transfected rats than in Adβgal-transfected rats. In addition, microinjection of tempol decreased blood pressure in the AdiNOS group, but not in the nontreated group. Furthermore, intracisternal infusion of tempol markedly attenuated the pressor response induced by AdiNOS transfection. In addition, the increased TBARS levels after AdiNOS transfection were significantly attenuated. Taken together, these results suggest that oxidative stress in the RVLM is increased in AdiNOS-transfected rats, and this increase might contribute to the pressor response evoked by iNOS transfection. NO might be trapped by superoxide anions. In support of this idea, we recently reported that increased reactive oxygen species in the RVLM contribute to the neural mechanisms of hypertension.[30]

An important finding of the present study was that blood pressure was increased after transfection of AdiNOS. The time course of the change in blood pressure was consistent with that of iNOS protein expression levels. This increase in blood pressure was nearly abolished by microinjection of aminoguanidine or SMT, a selective iNOS inhibitor, and partly inhibited by microinjection of L-NMMA, a nonselective NOS inhibitor. These results suggest that the pressor response that occurred after iNOS gene transfer was mediated by iNOS. If this is the case, then what caused the pressor response after iNOS production? We previously demonstrated that blood pressure decreased after transfection of AdeNOS into the RVLM.[19] eNOS and nNOS are constitutive NOS. Microinjection of L-NMMA in rats transfected with Adβgal elicited the pressor response, suggesting that NO produced by endogenous NOS in the RVLM, mainly nNOS, decreases blood pressure. In contrast, microinjection of aminoguanidine into the RVLM in Adβgal-transfected rats did not alter blood pressure, suggesting that endogenous iNOS in the RVLM does not affect blood pressure, at least in normotensive rats. In support of this finding, we demonstrated that expression levels of iNOS protein in the brain of WKY are very low compared with the aorta and heart and with stroke-prone spontaneously hypertensive rats.[13] HR did not change despite the fact that blood pressure was increased after iNOS gene transfection. This might be attributable to inhibition of the baroreflex control of HR. Blood pressure also returned to the control level after iNOS transfection into the RVLM, indicating that the cytotoxic effects of NO produced by iNOS in the present study are reversible. We transfected iNOS bilaterally into the RVLM. If RVLM neurons were irreversibly damaged, blood pressure would be expected to decrease to the level produced by spinal transection.[8]

The effects of NO in the RVLM on blood pressure regulation are controversial. NO in the RVLM is reported to reduce blood pressure by inhibiting sympathetic nerve activity;[6,12,47,48] but opposite results have also been reported.[49–51] In addition, it was reported that NO elicits a biphasic response that depends on the dose injected.[43] Most of these studies, however, were performed in anesthetized animals, and only acute effects of NO donors or nonselective NO blockers were examined. It is possible that NO donors such as sodium nitroprusside produce reactive oxygen species. To exclude the above-mentioned limitations, we demonstrated that transfection of adenovirus encoding constitutive eNOS in the RVLM reduces blood pressure via inhibition of the sympathetic nervous system and this effect is probably attributable to an increase in γ-amino-butyric acid (GABA) in the RVLM in conscious rats.[19] We used eNOS instead of nNOS, which is normally abundant in the CNS, because the purpose of that study was to increase NO production from constitutively expressed NOS. In support of these findings, a similar finding was obtained in the paraventricular nucleus of the hypothalamus[52] and RVLM.[16]

Recently, the contribution of nNOS or iNOS in the RVLM to blood pressure regulation was examined in propofol-anesthetized rats.[42] A selective inhibitor of nNOS, 7-nitroindazole, or selective antagonists of iNOS, aminoguanidine, N^6-(L-iminoethyl)-L-lysine, or SMT, were used in that study. The nNOS inhibitor reduced blood pressure and iNOS antagonists increased blood pressure, suggesting that endogenous NO produced by nNOS increases blood pressure and that produced by iNOS decreases blood pressure.[34] In a subsequent study, they explained that the different blood pressure responses evoked by nNOS and iNOS were attributable to differences in the amount of release of an excitatory neurotransmitter, L-glutamate, and an inhibitory neurotransmitter, GABA.[53] We do not yet have a clear explanation for the differences between their results and ours. Therefore, in the present study, we performed iNOS gene transfer into the RVLM in awake rats to clarify the role of iNOS in the RVLM. Our results raise another possibility that NO produced by iNOS enhances the production of reactive oxygen species, which influences the neuronal activity of the RVLM neurons.[30,53] Increased and sustained NO levels might lead to the formation of superoxide anions that react with NO to form peroxynitrite.[54] In support of this suggestion, nitrotyrosine staining in the RVLM was observed after transfection of AdiNOS as a peroxynitrite footprint. Indeed, lipopolysaccharide-induced NO generation results in an increase in oxidative stress in the rat liver and kidney and is inhibited by iNOS inhibitors.[55]

In summary, the present studies demonstrate that overexpression of iNOS in the RVLM elicits hypertension by activating the sympathetic nervous system, and these effects might be mediated by an increase in oxidative stress in the RVLM. An increase in iNOS expression levels occurs in some pathophysiological states, such as hypertension, heart failure, and endotoxin shock, and in aging.[22–28,41] Thus, it is conceivable that the increase in iNOS expression levels in the brain, particularly in the RVLM, occurs in those conditions, thereby modulating central sympathetic outflow resulting in blood pressure changes.

Acknowledgments

This work was supported by grants-in-aid for scientific research from the Ministry of Education, Science, Sports, and Culture (C13670721, C15590757), and by grants for research on auto-

nomic nervous system and hypertension from Kimura Memorial Heart Foundation/Pfizer Japan, Inc. We thank Drs Donald D. Heistad and Beverly L. Davidson (The University of Iowa Gene Transfer Vector Core, supported by the National Institutes of Health Grants and the Carver Foundation) for vector preparation.

References

1. Krukoff TL. Central actions of nitric oxide in regulation of autonomic functions. *Brain Res Rev.* 1999;30:52–65.
2. Persson PB. Modulation of cardiovascular control of mechanisms and their interaction. *Physiol Rev.* 1996;76:193–244.
3. Zanzinger J. Role of nitric oxide in the neural control of cardiovascular function. *Cardiovasc Res.* 1999;43:639–649.
4. Patel KP, Li Y-F, Hirooka Y. Role of nitric oxide in central sympathetic outflow. *Exp BiolMed.* 2001;226:814–824.
5. Zhang K, Mayhan WG, Patel KP. Nitric oxide within the paraventricular nucleus mediates changes in renal sympathetic nerve activity. *Am J Physiol Regul Integr Comp Physiol.* 1997;273:R864–R872.
6. Tseng CJ, Liu HY, Lin HC, Ger LP, Tung CS, Yen MH. Cardiovascular effects of nitric oxide in the brain stem nuclei of rats. *Hypertension.* 1996;27:36–42.
7. Lawrence AJ. Nitric oxide as a modulator of medullary pathways. *Clin Exp Pharmacol Physiol.* 1997;24:760–763.
8. Dampney RAL. Functional organization of central pathways regulating the cardiovascular system. *Physiol Rev.* 1994;74:323–364.
9. Guyenet PG. Role of the ventral medulla oblongata in blood pressure regulation. In: Loewy AD, Spyer KM, eds. *Central Regulation of Autonomic Functions.* New York: Oxford University Press;1990: 145–167.
10. Pilowski PM, Goodchild AK. Baroreceptor reflex pathways and neurotransmitters: 10 years on. *J Hypertens.* 2002;20:1675–1688.
11. Kishi T, Hirooka Y, Ito K, Sakai K, Shimokawa H, Takeshita A. Cardiovascular effects of overexpression of endothelial nitric oxide synthase in the rostral ventrolateral medulla in stroke-prone spontaneously hypertensive rats. *Hypertension.* 2002;39:264–268.
12. Kagiyama S, Tsuchihashi T, Abe I, Fujishima M. Enhanced depressor response to nitric oxide in the rostral ventrolateral medulla of spontaneously hypertensive rats. *Hypertension.* 1998;31:1030–1034.
13. Kishi T, Hirooka Y, Mukai Y, Shimokawa H, Takeshita A. Atorvastatin causes depressor and sympatho-inhibitory effects with upregulation of nitric oxide synthases in stroke-prone spontaneously hypertensive rats. *J Hypertens.* 2003;21:379–386.
14. Kishi T, Hirooka Y, Kimura Y, Sakai K, Ito K, Shimokawa H, Takeshita A. Overexpression of eNOS in RVLM improves impaired baroreflex control of heart rate in SHRSP. *Hypertension.* 2003;41:255–260.
15. Hirooka Y, Shigematsu H, Kishi T, Kimura Y, Ueta Y, Takeshita A. Reduced nitric oxide synthase in the brainstem contributes to enhanced sympathetic drive in rats with heart failure. *J Cardiovasc Pharmacol.* 2003;42:S111–S115.
16. Wang Y, Patel KP, Cornish KG, Channon KM, Zucker IH. nNOS gene transfer to RVLM improves baroreflex function in rats with chronic heart failure. *Am J Physiol.* 2003;285:H1660–H1667.
17. Hirooka Y. Adenovirus-mediated gene transfer into the brain stem to examine cardiovascular function: role of nitric oxide and Rho-kinase. *Prog Biophys Mol Biol.* 2004;84:233–249.
18. Hirooka Y, Kishi T, Sakai K, Shimokawa H, Takeshita A. Effect of overproduction of nitric oxide in the brain stem on the cardiovascular response in conscious rats. *J Cardiovasc Pharmacol.* 2003;41: S119–S126.
19. Kishi T, Hirooka Y, Sakai K, Shigematsu H, Shimokawa H, Takeshita A. Overexpression of eNOS in the RVLM causes hypotension and bradycardia via GABA release. *Hypertension.* 2001;38:896–901.
20. Hirooka Y, Sakai K, Kishi T, Ito K, Shimokawa H, Takeshita A. Enhanced depressor response to endothelial nitric oxide synthase gene transfer into the nucleus tractus solitarii of spontaneously hypertensive rats. *Hypertens Res.* 2003;26:325–331.
21. Sakai K, Hirooka Y, Matsuo I, Eshima K, Shigematsu H, Shimokawa H, Takeshita A. Overexpression of eNOS in NTS causes hypotension and bradycardia in vivo. *Hypertension.* 2000;36:1023–1028.
22. Chou T-C, Yen M-H, Li C-Y, Ding Y-A. Alterations of nitric oxide synthase expression with aging and hypertension in rats. *Hypertension.* 1998;31:643–648.
23. Hong H-J, Loh S-H, Yen M-H. Suppression of the development of hypertension by the inhibitor of inducible nitric oxide synthase. *Br J Pharmacol.* 2000;131:631–637.
24. Feng Q, Lu X, Jones DL, Shen J, Arnold JMO. Increased inducible nitric oxide synthase expression contributes to myocardial dysfunction and higher mortality after myocardial infarction in mice. *Circulation.* 2001; 104:700–704.
25. Yang B, Larson DF, Watson RR. Modulation of iNOS activity in age-related cardiac dysfunction. *Life Sci.* 2004;75:655–667.
26. Horinaka S, Kobayashi N, Mori Y, Yagi H, Onoda M, Matsuoka H. Expression of inducible nitric oxide synthase, left ventricular function and remodeling in Dahl salt-sensitive hypertensive rats. *Int J Cardiol.* 2003; 91:25–35.
27. Massion PB, Feron O, Balligand J-L. Nitric oxide and cardiac function: ten years after, and coming. *Circ Res.* 2003;93:388–398.
28. Briones AM, Alonso MJ, Hernanz R, Miguel M, Salaices M. Alterations of nitric oxide pathway in cerebral arteries from spontaneously hypertensive rats. *J Cardiovasc Pharmacol.* 2002;39:378–388.
29. Kato N, Yanaka K, Hyodo K, Homma K, Nagase S, Nose T. Stable nitroxide Tempol ameliorates brain injury by inhibiting lipid peroxidation in a rat model of transient focal cerebral ischemia. *Brain Res.* 2003;979: 188–193.
30. Kishi T, Hirooka Y, Kimura Y, Ito K, Shimokawa H, Takeshita A. Increased reactive oxygen species in rostral ventrolateral medulla contribute to neural mechanisms of hypertension in stroke-prone spontaneously hypertensive rats. *Circulation.* 2004;109:2357–2362.
31. Chu Y, Heistad DD. Gene transfer to blood vessels using adenoviral vectors. *Methods Enzymol.* 2002;346:253–276.
32. Gunnett CA, Lund DD, Brooks II RM, Faraci FM, Heistad DD. NO-dependent vasorelaxation is impaired after gene transfer of inducible NO-synthase. *Arterioscler Thromb Vasc Biol.* 2001;21:1281–1287.
33. Ooboshi H, Chu Y, Rios CD, Faraci FM, Davidson BL, Heistad DD. Altered vascular function after adenovirus-mediated overexpression of endothelial nitric oxide synthase. *Am J Physiol.* 1997;273: H265–H270.
34. Yamada K, Nabeshima T. Simultaneous measurement of nitrite and nitrate levels as indices of nitric oxide release in the cerebellum of conscious rats. *J Neurochem.* 1997;68:1234–1243.
35. Matsuo I, Hirooka Y, Hironaga K, Eshima K, Shigematsu H, Shihara M, Sakai K, Takeshita A. Glutamate release via NO production evoked by NMDA in the NTS enhances hypotension and bradycardia in vivo. *Am J Physiol.* 2001;280:R1285–R1291.
36. Zimmerman MC, Lazartigues E, Sharma RV, Davisson RL. Hypertension caused by angiotensin II infusion involves increased superoxide production in the central nervous system. *Circ Res.* 2004;95:210–216.
37. Gao L, Wang W, Li Y-L, Schultz HD, Liu D, Cornish KG, Zucker IH. Superoxide mediates sympathoexcitation in heart failure: roles of angiotensin II and NAD(P)H oxidase. *Circ Res.* 2004;95:937–944.
38. Kagiyama S, Tsuchihashi T, Abe I, Matsumura K, Fujishima M. Central infusion of L-arginine or superoxide dismutase does not alter arterial pressure in SHR. *Hypertens Res.* 2000;23:339–343.
39. Ito K, Hirooka Y, Kishi T, Kimura Y, Kaibuchi K, Shimokawa H, Takeshita A. Rho/Rho-kinase pathway in the brainstem contributes to hypertension caused by chronic nitric oxide synthase inhibition. *Hypertension.* 2004;43:156–162.
40. Sato K, Miyakawa K, Takeya M, Hattori R, Yui Y, Sunamoto M, Ichimori Y, Ushio Y, Takahashi K. Immunohistochemical expression of inducible nitric oxide synthase (iNOS) in reversible endotoxic shock studied by a novel monoclonal antibody against rat iNOS. *J Leukoc Biol.* 1995;57:36–44.
41. Murphy S, Simmons ML, Agullo L, Garcia A, Feinstein DL, Galea E, Reis DJ, Minc-Golomb D, Schwartz JP. Synthesis of nitric oxide in CNS glial cells. *TINS.* 1993;16:323–328.
42. Chan SHH, Wang L-L, Wang S-H, Chan JYH. Differential cardiovascular responses to blockade of nNOS or iNOS in rostral ventrolateral medulla. *Br J Pharmacol.* 2001;133:606–614.
43. Morimoto S, Sasaki S, Miki S, Kawa T, Nakamura K, Itoh H, Nakata T, Takeda K, Nakagawa M, Fushiki S. Nitric oxide is an excitatory modulator in the rostral ventrolateral medulla in rats. *Am J Hypertens.* 2000; 13:1125–1134.
44. Xia Y, Roman LJ, Masters BSS, Zweier JL. Inducible nitric-oxide synthase generates superoxide from the reductase domain. *J Biol Chem.* 1998;273:22635–22639.

45. Xia Y, Zweier JL. Superoxide and peroxynitrite generation from inducible nitric oxide synthase in macrophages. *Proc Natl Acad Sci USA*. 1997;94:6954–6958.
46. Wu F, Wilson JX, Tyml K. Ascorbate inhibits iNOS expression and preserves vasoconstrictor responsiveness in skeletal muscle of septic mice. *Am J Physiol*. 2003;285:R50–R56.
47. Kagiyama S, Tsuchihashi T, Abe I, Fujishima M. Cardiovascular effects nitric oxide in the rostral ventrolateral medulla of rats. *Brain Res*. 1997; 757:155–158.
48. Zanzinger J, Czachurski J, Seller H. Inhibition of basal and reflex-mediated sympathetic activity in the RVLM by nitric oxide. *Am J Physiol*. 1995;268:R958–R962.
49. Hirooka Y, Polson JW, Dampney RA. Pressor and sympathoexcitatory effects of nitric oxide in the rostral ventrofateral medulla. *J Hypertens*. 1996;14:1317–1324.
50. Martins-Pinge MC, Baraldi-Passy I, Lopes OU. Excitatory effects of nitric oxide within the rostral ventrolateral medulla of freely moving rats. *Hypertension*. 1997;30:704–707.
51. Chan SHH, Wang L-L, Chan JYH. Differential engagements of glutamate and GABA receptors in cardiovascular actions of endogenous nNOS or iNOS at rostral ventrolateral medulla of rats. *Br J Pharmacol*. 2003;138:584–593.
52. Li YF, Roy SK, Channon KM, Zucker IH, Patel KP. Effect of in vivo gene transfer of nNOS in the PVN on renal nerve disharge in rats. *Am J Physiol Heart Circ Physiol*. 2002;282:H594–H601.
53. Zanzinger J. Mechanisms of action of nitric oxide in the brain stem: role of oxidative stress. *Auton Neurosci*. 2002;98:24–27.
54. Boczkowski J, Lisdero CL, Lanone S, Samb A, Carreeas MC, Boveris A, Aubier M, Poderoso JJ. Endogenous peroxynitrite mediates mitochondrial dysfunction in rat diaphragm during endotoxemia. *FASEB J*. 1999;13:1637–1647.
55. Zhang C, Walker LM, Hinson JA, Mayeux PR. Oxidant stress in rat liver after lipopolysaccharide administration: effect of inducible nitric-oxide synthase inhibition. *J Pharmacol Exper Ther*. 2000;293: 968–972.

Extracorporeal Cardiac Shock Wave Therapy Markedly Ameliorates Ischemia-Induced Myocardial Dysfunction in Pigs in Vivo

Takahiro Nishida, MD; Hiroaki Shimokawa, MD; Keiji Oi, MD; Hideki Tatewaki, MD; Toyokazu Uwatoku, MD; Kohtaro Abe, MD; Yasuharu Matsumoto, MD; Noriyoshi Kajihara, MD; Masataka Eto, MD; Takehisa Matsuda, PhD; Hisataka Yasui, MD; Akira Takeshita, MD; Kenji Sunagawa, MD

Background—Prognosis of ischemic cardiomyopathy still remains poor because of the lack of effective treatments. To develop a noninvasive therapy for the disorder, we examined the in vitro and vivo effects of extracorporeal shock wave (SW) that could enhance angiogenesis.

Methods and Results—SW treatment applied to cultured human umbilical vein endothelial cells significantly upregulated mRNA expression of vascular endothelial growth factor and its receptor Flt-1 in vitro. A porcine model of chronic myocardial ischemia was made by placing an ameroid constrictor at the proximal segment of the left circumflex coronary artery, which gradually induced a total occlusion of the artery with sustained myocardial dysfunction but without myocardial infarction in 4 weeks. Thereafter, extracorporeal SW therapy to the ischemic myocardial region (200 shots/spot for 9 spots at 0.09 mJ/mm^2) was performed (n=8), which induced a complete recovery of left ventricular ejection fraction (51±2% to 62±2%), wall thickening fraction (13±3% to 30±3%), and regional myocardial blood flow (1.0±0.2 to 1.4±0.3 mL · min^{-1} · g^{-1}) of the ischemic region in 4 weeks (all $P<0.01$). By contrast, animals that did not receive the therapy (n=8) had sustained myocardial dysfunction (left ventricular ejection fraction, 48±3% to 48±1%; wall thickening fraction, 13±2% to 9±2%) and regional myocardial blood flow (1.0±0.3 to 0.6±0.1 mL · min^{-1} · g^{-1}). Neither arrhythmias nor other complications were observed during or after the treatment. SW treatment of the ischemic myocardium significantly upregulated vascular endothelial growth factor expression in vivo.

Conclusions—These results suggest that extracorporeal cardiac SW therapy is an effective and noninvasive therapeutic strategy for ischemic heart disease. (***Circulation.* 2004;110:3055-3061.**)

Key Words: angiogenesis ■ contractility ■ hibernation ■ ischemia ■ regional blood flow

Prognosis of ischemic cardiomyopathy without an indication for coronary intervention or coronary artery bypass grafting still remains poor because medication is the only therapy to treat the disorder.[1] Thus, it is imperative that an effective and noninvasive therapy for ischemic cardiomyopathy be developed. Although no medication or procedure used clinically has shown efficacy in replacing myocardial scar with functioning contractile tissue, it could be possible to improve the contractility of the hibernating myocardium by inducing angiogenesis.

It recently has been suggested that shock wave (SW) could enhance angiogenesis in vitro.[2] SW is a longitudinal acoustic wave, traveling with the speed in water of ultrasound through body tissue. It is a single pressure pulse with a short needle-like positive spike <1 μs in duration and up to 100 MPa in amplitude, followed by a tensile part of several microseconds with lower amplitude.[3] SW is known to exert the "cavitation effect" (a micrometer-sized violent collapse of bubbles inside and outside the cells)[3] and recently has been demonstrated to induce localized stress on cell membranes that resembles shear stress.[4] If SW-induced angiogenesis could be reproduced in vivo, it would provide a unique opportunity to develop a new angiogenic therapy that would not require invasive procedures such as open-chest surgery or catheter intervention. Therefore, the present study was designed to examine the possible beneficial effects of SW on ischemia-induced myocardial dysfunction in a porcine model of chronic myocardial ischemia in vivo.

Methods

This study was reviewed by the Committee on Ethics in Animal Experiments of Kyushu University and was carried out under the

Received May 5, 2003; de novo received June 2, 2004; accepted June 17, 2004.

From the Departments of Cardiovascular Surgery (T.N., H.T., N.K., M.E., H.Y.), Cardiovascular Medicine (K.O., H.S., T.U., K.A., Y.M., A.T., K.S.), and Biomedical Engineering (T.M.), and the 21st Century COE Program on Lifestyle-Related Diseases (H.S., T.M.), Kyushu University Graduate School of Medical Sciences, Fukuoka, Japan.

Correspondence to Hiroaki Shimokawa, MD, PhD, Department of Cardiovascular Medicine, Kyushu University Graduate School of Medical Sciences, 3-1-1 Maidashi, Higashi-ku, Fukuoka 812-8582, Japan. E-mail shimo@cardiol.med.kyushu-u.ac.jp

Circulation is available at http://www.circulationaha.org

DOI: 10.1161/01.CIR.0000148849.51177.97

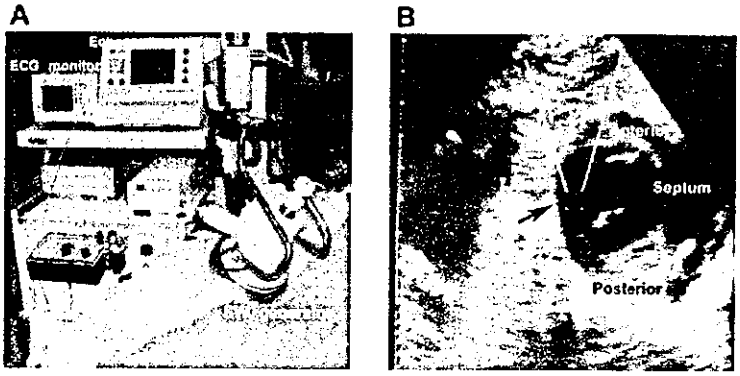

Figure 1. Extracorporeal cardiac SW therapy in action in a pig chronically instrumented with an ameroid constrictor. A, The machine is equipped with a SW generator and in-line echocardiography. The SW generator is attached to the chest wall when used. B, The SW pulse is easily focused on the ischemic myocardium under the guidance of echocardiography (black arrow).

Guidelines for Animal Experiments of Kyushu University and the Law (No. 105) and Notification (No. 6) of the Japanese Government.

Effect of SW on Human Umbilical Vein Endothelial Cells in Vitro

We purchased single-donor human umbilical vein endothelial cells (HUVECs) (Clonetics, Walkersville, Md) and cultured them in a complete endothelial medium (EBM-2 BulletKit, Clonetics). HUVECs were subcultured and used at passages 3 to 5 and were maintained in EBM-2. Twenty-four hours before the SW treatment, HUVECs (1×10^5) were resuspended in a 2-mL tube with EBM (Clonetics). We treated the HUVECs with 500 shots of SW at 4 different energy levels (0 [control], 0.02, 0.09, 0.18, and 0.35 mJ/mm^2) and stored them for 24 hours in the same medium before RNA extraction.

Ribonuclease Protection Assay

We analyzed equal amounts of mRNA by ribonuclease protection assay by means of the RiboQuant multiprobe template (PharMingen). Briefly, we hybridized RNA overnight with a ^{32}P-labeled RNA probe, which previously had been synthesized from the template set. We digested single-stranded RNA and free probe by ribonuclease A and T1. We then analyzed protected RNA on a 5% denaturing polyacrylamide gel. We analyzed several angiogenic factors, including vascular endothelial growth factor (VEGF) and its receptor, *fms*-like tyrosine kinase (Flt)-1, and angiopoietin and its receptor, tie-1, either by means of an NIH image or by means of autoradiography and subsequent quantification by densitometry (Alpha Innotech). For quantification, we normalized the signals for each sample of the blot with the corresponding signals of the housekeeping genes GAPDH and L32.

Porcine Model of Chronic Myocardial Ischemia

A total of 28 domestic pigs (25 to 30 kg in body weight) were used in this study. We anesthetized the animals with ketamine (15 mg/kg IM) and maintained anesthesia with an inhalation of 1.5% isoflurane for implantation of an ameroid constrictor, SW treatment, and euthanization. We opened the chest, suspended the pericardium and the left atrial appendage, revealed the left circumflex coronary artery (LCx), and put an ameroid constrictor around the proximal LCx to gradually induce a total occlusion of the artery in 4 weeks without causing myocardial infarction.[5,6] We also confirmed histologically that no myocardial necrosis had developed in the present porcine model (data not shown). This model is widely used to examine the effect of an angiogenic therapy in the ischemic hibernating myocardium.[5,6]

Extracorporeal Cardiac SW Therapy to Chronic Ischemic Myocardium

On the basis of the in vitro experiment, we applied a low energy of SW (0.09 mJ/mm2, ≈10% of the energy for the lithotripsy treatment) to 9 spots in the ischemic region (200 shots/spot) with the guidance of an echocardiogram equipped within a specially designed SW generator (Storz Medical AG) (Figure 1A). We were able to focus SW in any part of the heart under the guidance of echocardiography (Figure 1B). We applied SW to the ischemic myocardium in an R-wave–triggered manner to avoid ventricular arrhythmias. We performed the SW treatment (n=8) at 4 weeks after the implantation of an ameroid constrictor 3 times within 1 week, whereas animals in the control group (n=8) received the same anesthesia procedures 3 times a week but without the SW treatment. Because the SW treatment only requires the gentle compression of the generator to the chest wall, it is unlikely that this handling itself enhances angiogenesis in the ischemic myocardium.

Coronary Angiography and Left Ventriculography

After systemic heparinization (10 000 U/body), we performed coronary angiography and left ventriculography in a left oblique view with the use of a cineangiography system (Toshiba Medical). We semiquantitatively evaluated the extent of collateral flow to the LCx by the graded Rentrop score (0, no visible collateral vessels; 1, faint filling of side branches of the main epicardial vessel without filling the main vessel; 2, partial filling of the main epicardial vessel; 3, complete filling of the main vessel).[7] We also counted the number of visible coronary arteries in the LCx region. To compare the extent of collateral development at a given time, we selected the frame in which the whole left anterior descending coronary artery was first visualized.

Echocardiographic Evaluation

We performed epicardial echocardiographic studies at ameroid implantation (baseline) and at 4 and 8 weeks after the implantation of the constrictor (Sonos 5500, Agilent Technology). We calculated wall thickening fraction (WTF) by using the following formula: WTF = 100 × (end-systolic wall thickness − end-diastolic wall thickness) /end-diastolic wall thickness. We measured WTF when pigs were sedated, with and without dobutamine loading (15 $\mu g \cdot kg^{-1} \cdot min^{-1}$). Dobutamine was infused continuously from the ear vein, and WTF was measured after the hemodynamic condition was stabilized (in ≈5 minutes).

Measurement of Regional Myocardial Blood Flow

We evaluated regional myocardial blood flow (RMBF) with colored microspheres (Dye-Trak, Triton Technology) at ameroid implantation (baseline) and at 4 and 8 weeks after implantation.[8] We injected microspheres through the left atrium and aspirated a reference arterial blood sample from the descending aorta at a constant rate of 20 mL/min for 60 seconds using a withdrawal pump. We extracted microspheres from the left ventricular (LV) wall and blood samples by potassium hydroxide digestion, extracted the dyes from the spheres with dimethylformamide (200 μL), and determined their concentrations by spectrophotometry.[8] We calculated myocardial blood flow ($mL \cdot min^{-1} \cdot g^{-1}$) of the endocardial and epicardial lateral LV wall (the LCx region).

Analysis of Cardiac Enzymes

We measured serum concentrations of cardiac troponin T and creatinine kinase (CK)–MB by using chemiluminescence immuno-

assay before the SW treatment and at 4, 5 (2 hours after the SW treatment), and 8 weeks after ameroid implantation.

Factor VIII Staining

We treated paraffin-embedded sections with a rabbit anti-factor VIII antibody (N1505, Dako, Copenhagen, Denmark). We counted the number of factor VIII–positive cells in the endocardial and epicardial wall in 10 fields of the LCx region in each heart at 400× magnification.

Real-Time Polymerase Chain Reaction

To examine the effect of SW treatment on the ischemic myocardium in vivo, the animals with an ameroid constrictor were euthanized 1 week after the SW treatment. Total RNA was isolated from rapidly frozen ischemic LV wall (LCx region) after 3 SW treatments and was reverse transcribed. Quantification of VEGF and its receptor Flt-1 was performed by amplification of cDNA with an ABI Prism 7000 real-time thermocycler.

Western Blot Analysis for VEGF

We performed Western blot analysis for VEGF. Western blot analysis for VEGF was performed with and without 3 SW treatments. Three sections from the ischemic LV wall (LCx region) were measured. The regions containing VEGF proteins were visualized by electrochemiluminescence Western blotting luminal reagent (Santa Cruz Biotechnology). The extent of the VEGF was normalized by that of β-actin.

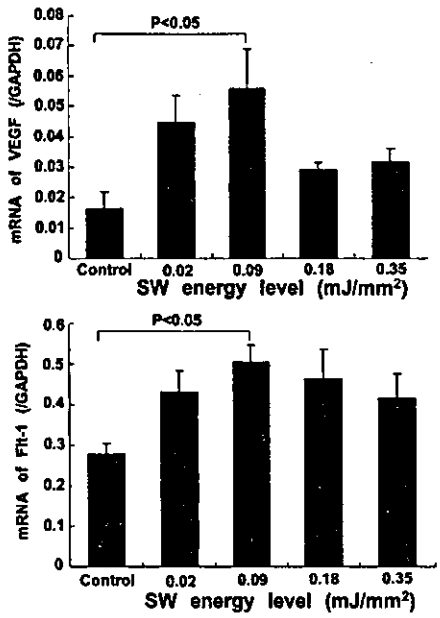

Figure 2. SW treatment upregulated mRNA expression of VEGF (A) and Flt-1 (B) in HUVECs in vitro with a maximum effect noted at 0.09 mJ/mm². Results are expressed as mean±SEM (n=10 each).

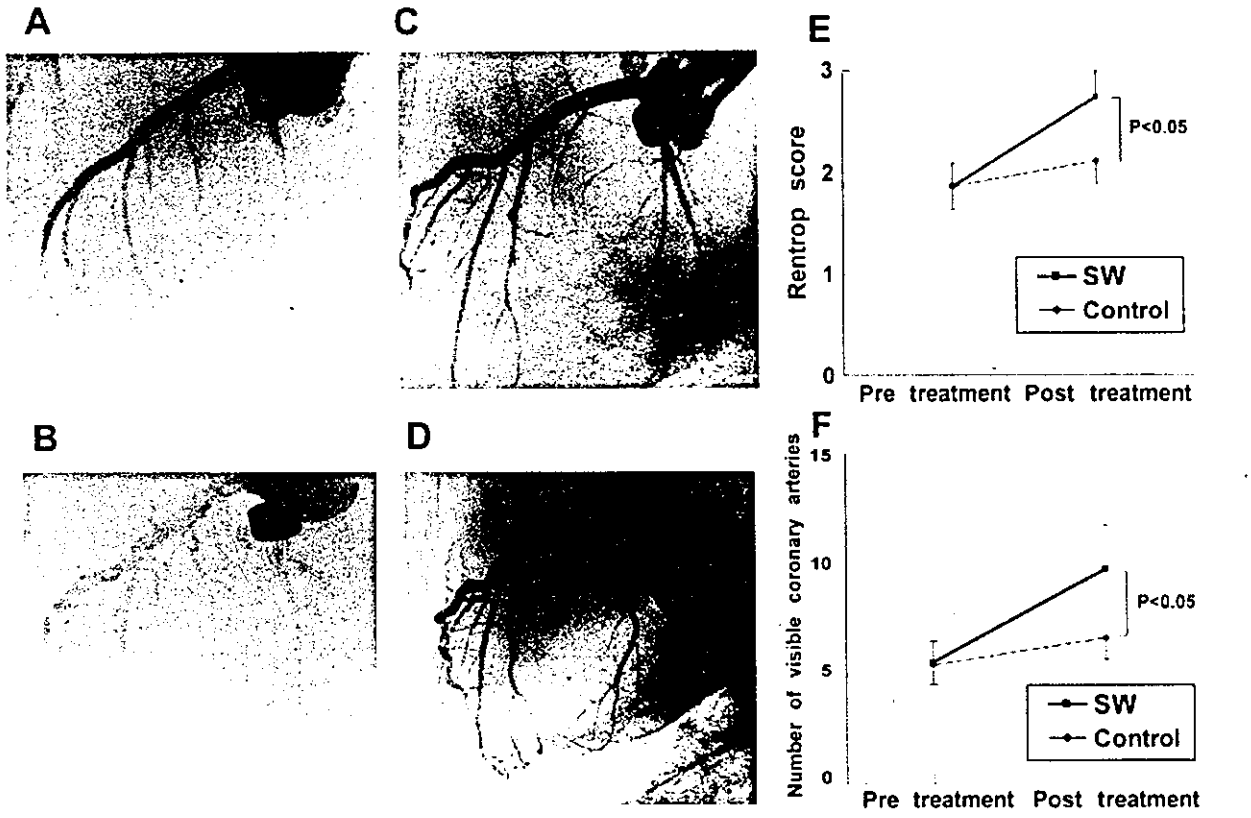

Figure 3. Extracorporeal cardiac SW therapy enhances coronary angiogenesis in vivo. A and C, Four weeks after the implantation of an ameroid constrictor, LCx was totally occluded and was perfused via collateral vessels with severe delay in both the control group (A) and the SW group (before SW therapy) (C). B and D, Four weeks after the first coronary angiography, no significant change in coronary vessels was noted in the control group (B), whereas a marked development of visible coronary vessels was noted in the SW group (D). E and F, Four weeks after the first coronary angiography, no significant increase in the Rentrop score (E) or visible coronary arteries from LCx (F) was noted in the control group, whereas increased Rentrop score and a marked development of visible coronary vessels were noted in the SW group. Results are expressed as mean±SEM (n=8 each).

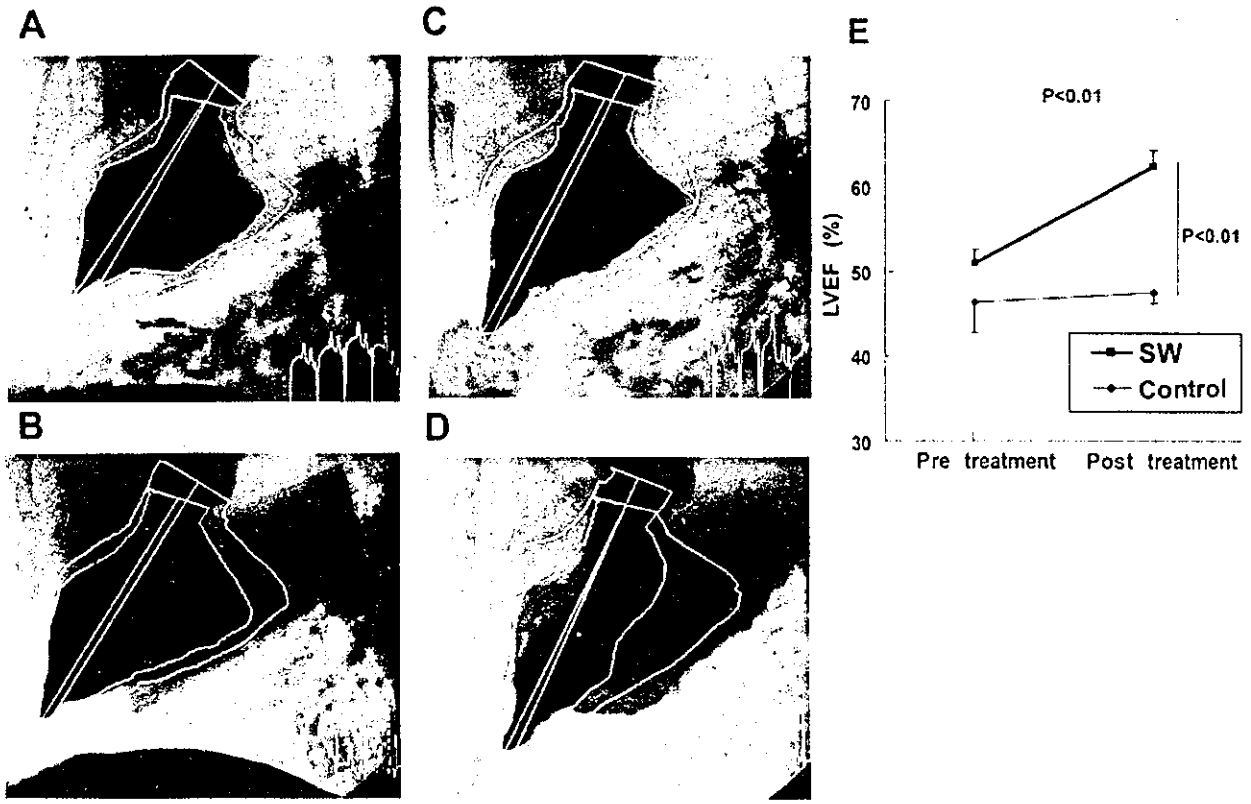

Figure 4. Extracorporeal cardiac SW therapy improves ischemia-induced myocardial dysfunction in vivo. A and C, Four weeks after the implantation of an ameroid constrictor, LV wall motion of the LCx (posterolateral) region was reduced in both the control (A) and the SW group (before the SW therapy) (C). B and D, Four weeks after the first left ventriculography, no significant change in LV wall motion was noted in the control group (B), whereas marked recovery was noted in the SW group (D). E, The SW therapy normalized left ventricular ejection fraction in the SW group but not in the control group. Results are expressed as mean±SEM (n=8 each).

Statistical Analysis

Results are expressed as mean±SEM. We determined statistical significance by analysis of variance for multiple comparisons. A value of $P<0.05$ was considered to be statistically significant.

Results

Effect of SW on mRNA Expression of VEGF and Flt-1 in HUVECs

SW treatment significantly upregulated mRNA expression of VEGF and its receptor Flt-1 in HUVECs, with a maximum effect noted at 0.09 mJ/mm^2 (Figure 2).

Effects of Extracorporeal Cardiac SW Therapy on Angiogenesis and Ischemia-Induced Myocardial Dysfunction

Four weeks after ameroid implantation, coronary angiography demonstrated a total occlusion of the LCx, which was perfused via collateral vessels with severe delay in both the control (Figure 3A) and the SW groups (Figure 3C). At 8 weeks after ameroid implantation (4 weeks after SW therapy), the SW group (Figure 3D), but not the control group (Figure 3B), had a marked development of coronary collateral vessels in the ischemic LCx region, an increased Rentrop score (Figure 3E), and an increased number of visible coronary arteries in the region (Figure 3F). Similarly, at 4 weeks, left ventriculography demonstrated an impaired left ventricular ejection fraction in both groups (Figure 4A, 4C, and 4E), whereas at 8 weeks, left ventricular ejection fraction was normalized in the SW group but remained impaired in the control group (Figure 4B, 4D, and 4E).

Effects of Extracorporeal Cardiac SW Therapy on Regional Myocardial Function and Myocardial Blood Flow

We serially measured WTF of the LCx region (lateral wall of the LV) by epicardiac echocardiography. At 4 weeks, we observed a significant reduction in WTF (%) in both groups (13±2 in the control group and 13±3 in the SW group; Figure 5A). At 8 weeks, however, the SW treatment markedly improved WTF in the SW group (30±3) but not in the control group (9±2) under control conditions (Figure 5A). Under dobutamine-loading conditions, which mimicked exercise conditions, WTF was further reduced at 4 weeks after the ameroid implantation in both groups (16±3 in the control and 18±2 in the SW groups), however, at 8 weeks, WTF was again markedly ameliorated only in the SW group (31±2) but not in the control group (16±4) (Figure 5B).

At 4 weeks, RMBF in the endocardium and epicardium (mL · min^{-1} · g^{-1}) was equally decreased in both groups (1.0±0.3 and 0.9±0.2 in the control group and 1.0±0.2 and 0.9±0.2 in the SW group, respectively). The SW treatment again improved RMBF in the endocardium (0.6±0.1 in the

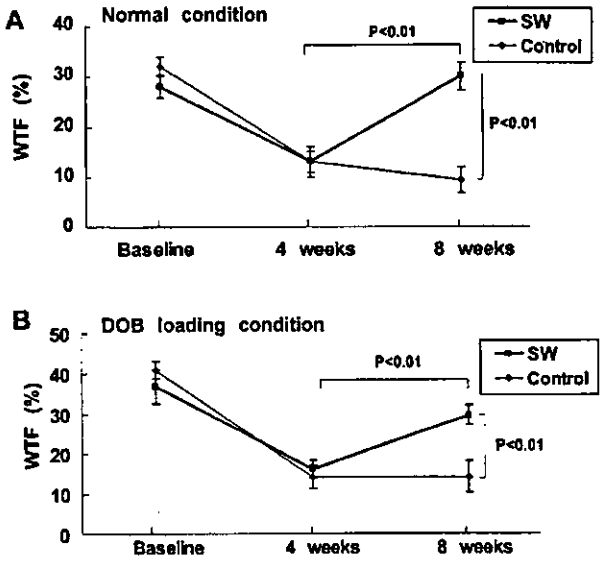

Figure 5. Extracorporeal cardiac SW therapy improves regional myocardial function in vivo. SW therapy induced a complete recovery of WTF of the ischemic lateral wall under control conditions (A) and under dobutamine (DOB) loading conditions (B). Results are expressed as mean±SEM (n=8 each).

control group and 1.4±0.3 in the SW group, $P<0.05$; Figure 6A) as well as in the epicardium (0.7±0.2 in the control group and 1.5±0.2 in the SW group, $P<0.05$; Figure 6B).

Effects of Extracorporeal Cardiac SW Therapy on Capillary Density and VEGF Expression in the Ischemic Myocardium

Factor VIII staining showed that the number of factor VIII–positive capillaries was increased in the SW group compared with the control group (Figure 7A and 7B). Quantitative analysis demonstrated that the number of capillaries was significantly higher in the SW group in both the endocardium (840±26 in the control group and 1280±45 in the SW group, $P<0.05$; Figure 7C) and the epicardium (820±30 in the control group and 1200±22 in the SW group, $P<0.05$; Figure 7D). RT-PCR analysis and Western blotting demonstrated a significant upregulation of VEGF mRNA expression (8.0±6 in the control group and 32±8 in the SW group, $P<0.05$; Figure 8A) and protein expression (2.23-fold increase in the SW groups, $P<0.05$; Figure 8B) after the SW treatment to the ischemic myocardium in vivo.

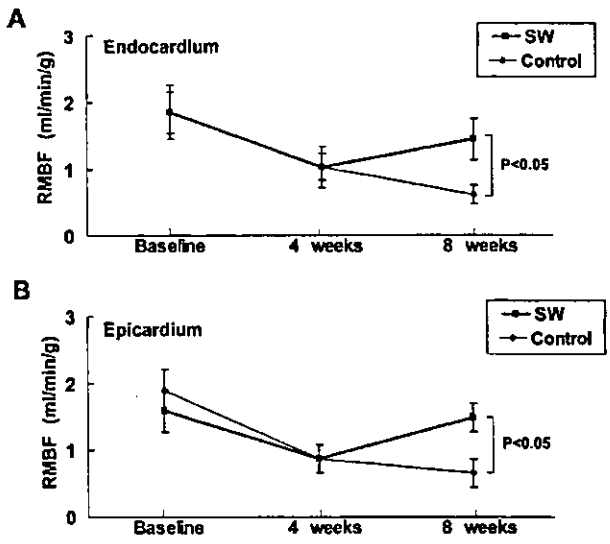

Figure 6. Extracorporeal cardiac SW therapy improves RMBF in vivo. SW therapy significantly increased RMBF, assessed by colored microspheres in both the endocardium (A) and the epicardium (B). Results are expressed as mean±SEM (n=8 each).

Side Effects of Extracorporeal Cardiac SW Therapy

All animals treated with the SW therapy were alive and showed no arrhythmias as assessed by 24-hour Holter ECG during and after the treatment (n=3; data not shown). There also was no myocardial cell damage as assessed by serum concentrations of CK-MB (ng/mL); the values before the SW treatment and at 4, 5 (2 hours after the SW treatment), and 8 weeks after the ameroid implantation were 5.0±0.6, 6.2±0.5, 5.5±0.2, and 7.1±0.9 in the control group and 5.1±0.2, 7.7±0.6, 6.1±0.6, and 6.4±0.4 in the SW group, respectively (n=6 each). The serum concentrations of troponin T were not detected in most cases in both groups. No significant differences were noted in hemodynamic variables (eg, heart rate or blood pressure) between the 2 groups (data not shown).

Discussion

The novel finding of the present study is that the extracorporeal cardiac SW therapy enhances angiogenesis in the ischemic myocardium and normalizes myocardial function in a porcine model of chronic myocardial ischemia in vivo. To the best of our knowledge, this is the first report that demonstrates the potential usefulness of extracorporeal cardiac SW therapy as a noninvasive treatment of chronic myocardial ischemia.

Extracorporeal Cardiac SW Therapy as a Novel Strategy for Ischemic Cardiomyopathy

Because of the poor prognosis of ischemic cardiomyopathy,[1,9] it is crucial to develop an alternative therapy for ischemia-induced myocardial dysfunction. To accomplish effective angiogenesis, it is mandatory to upregulate potent angiogenesis ligands, such as VEGF, and their receptors.[9,10] Furthermore, in the clinical setting, the goal for the treatment of ischemic cardiomyopathy should include not only enhancement of angiogenesis but also recovery of ischemia-induced myocardial dysfunction. In the present study, we were able to demonstrate that SW treatment (1) normalized global and regional myocardial functions as well as RMBF of the chronic ischemic region without any adverse effects in vivo, (2) increased vascular density in the SW-treated region, and (3) enhanced mRNA expression of VEGF and its receptor Flt-1 in HUVECs in vitro and VEGF production in the ischemic myocardium in vivo. Thus, SW-induced upregulation of the endogenous angiogenic system may offer a novel and promising noninvasive strategy for the treatment of ischemic heart disease.

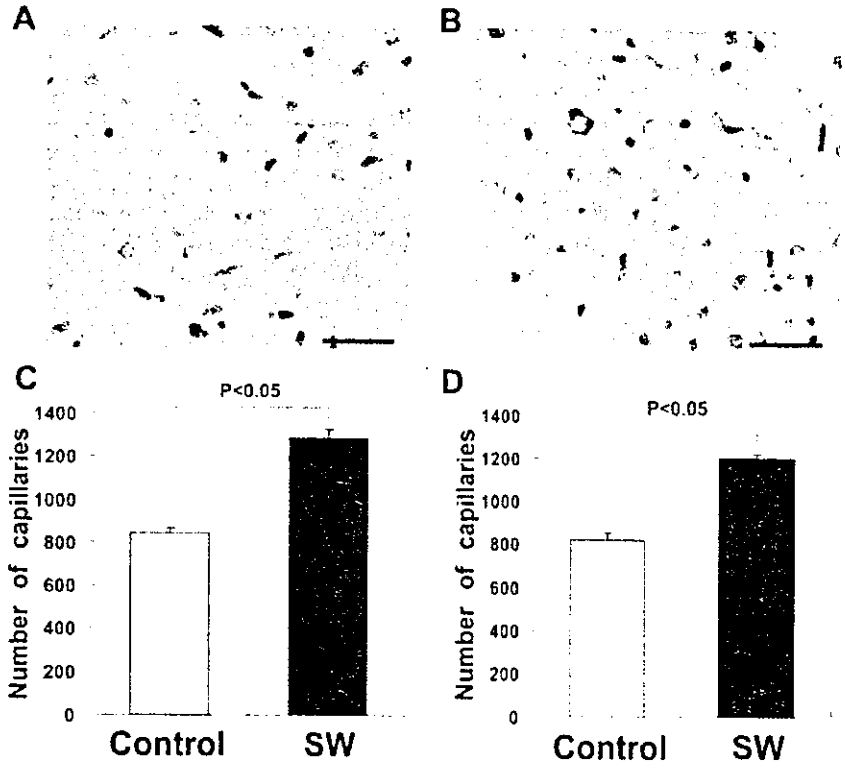

Figure 7. Extracorporeal cardiac SW therapy increases the density of factor VIII–positive capillaries in the ischemic myocardium. A and B, Factor VIII staining of the LCx region from the control (A) and the SW group (B). Scale bar represents 20 μm. C and D, Capillary density was significantly greater in the SW group (SW) than in the control group (Control) in both the endocardium (C) and the epicardium (D). Results are expressed as mean±SEM (n=6 each).

Advantages of Extracorporeal Cardiac SW Therapy

Recent attempts to enhance angiogenesis in the ischemic organs include gene therapy and bone marrow cell transplantation therapy. The main purpose of gene therapy is to induce overexpression of a selected angiogenic ligand (eg, VEGF) that leads to angiogenesis in the ischemic region. Although phase 1 trials of gene transfer of plasmid DNA encoding VEGF demonstrated safety and clinical benefit for the treatment of ischemic limb and heart,[11–13] gene therapy for ischemic cardiomyopathy is still at a preclinical stage. Bone marrow cell transplantation therapy, which depends on adult stem cell plasticity, also may be a useful strategy for angiogenesis because endothelial progenitor cells could be isolated from circulating mononuclear cells in humans and could be shown to be incorporated into neovascularization.[14] However, the need for invasive delivery of those cells to the ischemic myocardium may severely limit its usefulness in clinical situations.

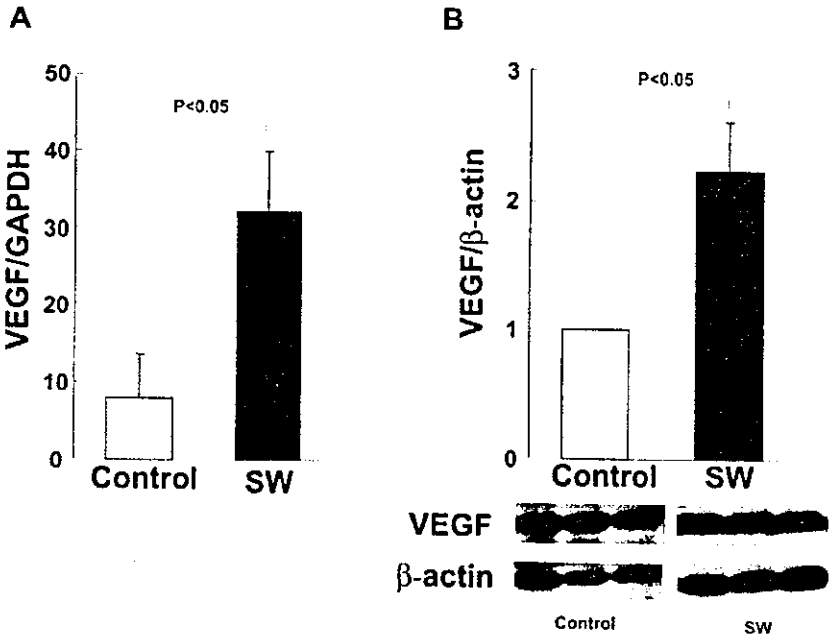

Figure 8. SW treatment upreglated mRNA (A) and protein (B) expression of VEGF in the ischemic myocardium (n=5 each).

A major advantage of the extracorporeal cardiac SW therapy over these 2 strategies is shown by the fact that it is quite noninvasive and safe, without any adverse effects. If necessary, we could repeatedly treat patients (even outpatients) with SW therapy because no surgery, anesthesia, or even catheter intervention is required for the treatment. This is an important factor in determining the clinical usefulness of angiogenic therapies in patients with ischemic cardiomyopathy. Thus, the extracorporeal cardiac SW therapy appears to be an applicable and noninvasive treatment for ischemic heart disease. Indeed, the SW treatment itself already has been clinically established as an effective and safe treatment for lithotripsy and chronic plantar fasciitis.[15,16] Our present results indicate that SW therapy, at ≈10% of the energy needed for lithotripsy treatment, is effective for in vivo angiogenesis in the ischemic heart.

Mechanisms for SW-Induced Angiogenesis

When a SW hits tissue, cavitation (a micrometer-sized violent collapse of bubbles) is induced by the first compression by the positive pressure part and the expansion with the tensile part of a SW.[3] Because the physical forces generated by cavitation are highly localized, SW could induce localized stress on cell membranes, as altered shear stress affects endothelial cells.[17] Recent reports have demonstrated the biochemical effects of SW, including hyperpolarization and Ras activation,[18] nonenzymatic nitric oxide synthesis,[19] and induction of stress fibers and intercellular gaps.[20] Although precise mechanisms for the SW-induced biochemical effects remain to be examined, these mechanisms may be involved in the underlying mechanisms for SW-induced angiogenesis. Indeed, Wang et al[21] reported that SW induces angiogenesis of the Achilles tendon–bone junction in dogs.

We were able to demonstrate that the SW treatment upregulated mRNA expression of VEGF and its receptor Flt in HUVECs in vitro and VEGF expression in the ischemic myocardium in vivo. Because the VEGF-Flt system is essential in initiating vasculogenesis and/or angiogenesis,[22] this effect of SW could explain, at least in part, the underlying mechanisms for SW-induced angiogenesis. It should be noted, however, that we showed only the upregulation of VEGF and Flt and that the effect of SW on signal transduction after receptor–ligand interaction still remains to be clarified. In addition, we need to fully elucidate the mechanisms for the SW-induced complete recovery of ischemia-induced myocardial dysfunction, although the increased myocardial blood flow caused by the SW treatment appears to play a primary role for the improved myocardial function. Further studies are required to determine the precise molecular mechanism for SW-induced angiogenesis and recovery of myocardial function.

In summary, we were able to demonstrate that noninvasive extracorporeal cardiac SW therapy effectively increases RMBF and normalizes ischemia-induced myocardial dysfunction without any adverse effects. Thus, extracorporeal cardiac SW therapy may be an effective, safe, and noninvasive therapy for ischemic cardiomyopathy.

Acknowledgments

This study was supported in part by a grant from the 21st Century COE Program and grants-in-aid from the Japanese Ministry of Education, Culture, Sports, Science, and Technology, Tokyo, Japan (Nos. 12032215, 12470158, 12877114, 13307024, 13557068), and the Japanese Ministry of Health, Labor, and Welfare, Tokyo, Japan. We thank Dr Ernest H. Marlinghaus, Storz Medical AG, Switzerland, for valuable discussion about our study, and Prof S. Mohri at the Center of Biomedical Research, Kyushu University Graduate School of Medical Sciences, for cooperation in this study.

References

1. Jessup M, Brozena S. Heart failure. *N Engl J Med*. 2003;348:2007–2018.
2. Gutersohn A, Caspari G. Shock waves upregulate vascular endothelial growth factor m-RNA in human umbilical vascular endothelial cells. *Circulation*. 2000;102(suppl):18.
3. Apfel RE. Acoustic cavitation: a possible consequence of biomedical uses of ultrasound. *Br J Cancer*. 1982;45(suppl):140–146.
4. Maisonhaute E, Prado C, White PC, et al. Surface acoustic cavitation understood via nanosecond electrochemistry, part III: shear stress in ultrasonic cleaning. *Ultrason Sonochem*. 2002;9:297–303.
5. O'Konski MS, White FC, Longhurst J, et al. Ameroid constriction of the proximal left circumflex coronary artery in swine: a model of limited coronary collateral circulation. *Am J Cardiovasc Pathol*. 1987;1:69–77.
6. Roth DM, Maruoka Y, Rogers J, et al. Development of coronary collateral circulation in left circumflex ameroid–occluded swine myocardium. *Am J Physiol*. 1987;253:H1279–1288.
7. Rentrop KP, Cohen M, Blanke H, et al. Changes in collateral channel filling immediately after controlled coronary artery occlusion by an angioplasty balloon in human subjects. *J Am Coll Cardiol*. 1985;5:587–592.
8. Prinzen FW, Bassingthwaighte JB. Blood flow distributions by microsphere deposition methods. *Cardiovasc Res*. 2000;45:13–21.
9. Carmeliet P, Ferreira V, Breier G, et al. Abnormal blood vessel development and lethality in embryos lacking a single VEGF allele. *Nature*. 1996;380:435–439.
10. Ferrara N, Carver-Moore K, Chen H, et al. Heterozygous embryonic lethality induced by targeted inactivation of the VEGF gene. *Nature*. 1996;380:439–442.
11. Isner JM, Pieczek A, Schainfeld R, et al. Clinical evidence of angiogenesis after arterial gene transfer of phVEGF165 in patient with ischaemic limb. *Lancet*. 1996;348:370–374.
12. Baumgartner I, Pieczek A, Manor O, et al. Constitutive expression of phVEGF165 after intramuscular gene transfer promotes collateral vessel development in patients with critical limb ischemia. *Circulation*. 1998;97:1114–1123.
13. Losordo DW, Vale PR, Symes JF, et al. Gene therapy for myocardial angiogenesis: initial clinical results with direct myocardial injection of phVEGF165 as sole therapy for myocardial ischemia. *Circulation*. 1998;98:2800–2804.
14. Asahara T, Murohara T, Sullivan A, et al. Isolation of putative progenitor endothelial cells for angiogenesis. *Science*. 1997;275:964–966.
15. Auge BK, Preminger GM. Update on shock wave lithotripsy technology. *Curr Opin Urol*. 2002;12:287–290.
16. Weil LS Jr, Roukis TS, Weil LS, et al. Extracorporeal shock wave therapy for the treatment of chronic plantar fasciitis: indications, protocol, intermediate results, and a comparison of results to fasciotomy. *J Foot Ankle Surg*. 2002;41:166–172.
17. Fisher AB, Chien S, Barakat AI, et al. Endothelial cellular response to altered shear stress. *Am J Physiol*. 2001;281:L529–L533.
18. Wang FS, Wang CJ, Huang HJ, et al. Physical shock wave mediates membrane hyperpolarization and Ras activation for osteogenesis in human bone marrow stromal cells. *Biochem Biophys Res Commun*. 2001;287:648–655.
19. Gotte G, Amelio E, Russo S, et al. Short-time non-enzymatic nitric oxide synthesis from L-arginine and hydrogen peroxide induced by shock waves treatment. *FEBS Lett*. 2002;520:153–155.
20. Seidl M, Steinbach P, Worle K, et al. Induction of stress fibres and intercellular gaps in human vascular endothelium by shock-waves. *Ultrasonics*. 1994;32:397–400.
21. Wang CJ, Huang HY, Pai CH. Shock wave–enhanced neovascularization at the tendon-bone junction: an experiment in dogs. *J Foot Ankle Surg*. 2002;41:16–22.
22. Millauer B, Wizigmann-Voos S, Schnurch H, et al. High affinity VEGF binding and developmental expression suggest Flk-1 as a major regulator of vasculogenesis and angiogenesis. *Cell*. 1993;72:835–846.